



## ELASTOSTATIC ANALYSIS OF THE SPATIAL FGM STRUCTURES

MURÍN, J.<sup>1</sup>, AMINBAGHAI, M.<sup>2</sup>, HRABOVSKÝ, J.<sup>1</sup>

<sup>1</sup>*Slovak University of Technology in Bratislava, Faculty of Electrical Engineering and Information Technology, Ilkovicova 3, 812 19 Bratislava, Slovakia, email: justin.murin@stuba.sk*

<sup>2</sup>*Institute for Mechanics of Materials and Structures, Karlsplatz 13, A-1040 Vienna, Austria, e-mail: mehdi.aminbaghai@tuwien.ac.at*

**Abstract:** In this contribution, results of elastostatic analysis of spatial composite beam structures are presented using our new beam finite element of double symmetric cross-section made of a Functionally Graded Material (FGM). Material properties of the real beams vary continuously in the longitudinal direction while variation with respect to the transversal and lateral directions is assumed to be symmetric in a continuous or discontinuous manner. Continuously longitudinal varying spatial Winkler elastic foundations (except the torsional foundation) and the effect of axial and shear forces are considered as well. Homogenization of spatially varying material properties to effective quantities with a longitudinal variation is done by the multilayer method (MLM). For the homogenized beam finite element the local stiffness matrix is established by means of the transfer matrix method. By the conventional finite element procedure, the global element stiffness matrix and the global system of equation for the beam structure are established for calculation of the global displacement vector. The secondary variables (internal forces and moments) are then calculated by means of the transfer relations on the real beams. Further, the mechanical stress in the real beams are calculated. Finally, the numerical experiments are carried out concerning the elastic-static analysis of the single FGM beams and beam structures in order to show the possibilities of our approach.

**KEYWORDS:** 3D FGM beam, spatially varying material properties, elastostatic analysis

### 1 Introduction

Important classes of structural components, where FGM is used, are beams and beam structures. FGM beams play an important role not only in classical structural applications, but we can find many applications in thermal, electric-thermal or electric-thermal-structural systems (e.g. micro-electro-mechanical systems (MEMS) as sensors and actuators and other mechatronic devices). In all these applications, using new materials like FGM can greatly improve the efficiency of the systems. FGM is built as a mixture of two or more constituents whose particles have almost the similar form and dimensions (powder, plasma particles, etc.). The continuous or multilayered variation of macroscopic material properties can be caused by varying the volume fraction of the constituents and with varying the constituents material properties (e.g. by a non-homogeneous temperature field). In the literature a huge amount of papers can be found which deal with modeling and simulation of static and dynamic problems of FGM beams. In [1], a review of the principal developments in FGM is processed with an emphasis on the recent work published since 2000. A current state in the elasto-static analysis of the FGM beam can be particularly documented by following papers: In [2], bending and free vibration of FGM beams resting on Winkler – Pasternak elastic foundation based on the two-dimensional theory of elasticity are presented. Exponentially varying material properties along the thickness direction were considered. In [3], high-order flexural theories for short functionally graded symmetric beams under three-point bending are presented. Transversal continuous variation of material properties was considered. In [4], displacement field based

on higher order shear deformation theory is implemented. FGM beams with variation of volume fractions of constituents based on power law exponent were considered. In [5], several axiomatic refined theories are proposed for the linear static analysis of beams made of materials whose properties are graded along one or two directions. In [6], the analysis of the large deformation of a non-linear planar cantilever FGM beam is made. In [7], a novel analytic approach is presented to solve the buckling instability of Euler – Bernoulli columns with arbitrarily axial inhomogeneity and/or varying cross-section. In [8], a size-dependent formulation is presented for Timoshenko FGM beams. The formulation is developed through the modified couple stress theory. In [9], non-linear static analysis of a cantilever Timoshenko beam composed of FGM under non-follower transversal uniformly distributed load is studied with large displacements and rotations. Material properties change in the thickness direction according the power-law function. In [10], an investigation of the dynamic stability of functionally graded ordinary beam and functionally graded sandwich beam on Winkler's foundation is presented. The material properties are assumed to follow both exponential and power law. In [11], a closed-form solution is obtained for the nonlinear static response of beams made of FGM subjected to uniform in-plane thermal loading. Transversal variation of the material properties has been considered. In [12], using the energy equivalence principle, a general expression is derived for the static shear correction factor in FGM beams. In [13], relationship between bending solutions of FGM Timoshenko beam and homogeneous Euler-Bernoulli beam is studied. In [14], the equation of large deflection of FGM beam subjected arbitrary loading conditions is derived. The longitudinal variation of elasticity modulus is assumed. In [15], the direct approach to the theory of rods and beams is employed. Non-homogeneous, composite and FGM beams made of isotropic or orthotropic materials have been considered. In [16], evaluation of static and dynamic behavior of FGM ordinary beam and FGM sandwich is presented. Transversal variation of material properties is considered. In [17], a symplectic framework for the analysis of plane problems of bi-directional FGM beam, in which the elastic modulus varies exponentially both along the longitudinal and transverse coordinates while the Poisson's ratio remains constant. In [18], thermal buckling and post-buckling of FGM Timoshenko beams resting on non-linear elastic foundation are examined. In [19], the bending, buckling and free vibration responses of Timoshenko micro-beams made of FGM with transversal variation of material properties is presented. In [20], nonlinear bending analysis of FGM beams based on physical neutral surface and high order shear deformation theory are investigated. Transversal variation of material properties is considered. In [21], bending solutions of Timoshenko FGM beams are derived analytically in terms of the homogeneous Euler-Bernoulli beams. In [22], stability of FGM micro-beam with transversal variation of material properties, subjected to nonlinear electrostatic pressure and thermal changes, is studied. In [23], elastoplastic analysis of micro FGM beam based on mechanism-based strain gradient plasticity theory is presented. Transverse variation of material properties has been assumed. In [24], based on modified couple stress theory, a FGM micro beam under electrostatic forces is studied. Variation of material properties through beam thickness was considered. In [25], the buckling behavior of size-dependent FGM micro beams with transverse variation of material properties is investigated. In [26], a curved micro beam model made of FGM is developed based on the strain gradient elasticity theory and n shear deformation theory. The material properties vary in the thickness direction and are estimated through Mori-Tanaka homogenization technique. In [27], thermal post-buckling and non-linear vibration behaviors of FGM are analyzed. Material properties are assumed to be temperature dependent and vary along the beam thickness. In [28], a unified and self-consistent treatment of a FGM micro beam, with varying thermal conductivity subjected to non-uniform and uniform temperature field, is provided. In [29], the large amplitude vibration, nonlinear bending and thermal postbuckling of FGM beams resting on an elastic

foundation in thermal environments is investigated. In [30], a higher order shear deformation beam theory is developed for static and free vibration analysis of FGM beams. In [31], geometrically nonlinear analysis of planar beam and frame structures made of FGM by using the finite element method is presented. In [32], a model of FGM beams resting on nonlinear elastic foundation is put forward by physical neutral surface and high-order shear deformation theory. In [33], a large deflection of nonlinearly elastic FGM beams is presented. Transverse variation of material properties is assumed. In [34], the postbuckling analysis of a nonlinear beam composed of axial functionally graded material is investigated. In [35], the double cantilever beam model is extended to FGM based on two-dimensional theory of elasticity. In [36], static analyses of FGM beams by various theories and finite elements are presented. In [37], a new beam finite element is developed to study the thermos-elastic behavior of FGM beam structures. The element is based on the first-order shear deformation theory and its accounts for varying elastic and thermal properties along its thickness. [38], dynamic characteristics of a functionally graded beam with axial or transversal material gradation along the thickness on the power law have been studied with a semi-analytical method.

In [39, 40, 41], we present an analysis of free vibration of a single 2D FGM beam with continuous planar polynomial variation of material properties (in axial and transversal direction) by a fourth-order differential equation of the second order beam theory. The aim of this publication was to present a new concept for expanding the second order bending beam theory considering the shear deformation according to Timoshenko beam theory. The shear deformation effect in FGM beams with planar continuous variation of material properties is there originally included by means of the average shear correction factor that has been obtained by an integration of the shear correction function [42]. The continuous polynomial variation of the effective elasticity modulus and mass density is considered by continuous polynomial spatial variation of both the volume fraction and material properties of the FGM constituents. The choice of a polynomial gradation of material properties enables an easier integration of the derived differential equation and allows to model practically realizable variations of material properties. The effect of consistent inertia and rotary inertia and the effect of axial forces were taken into account as well.

As mentioned above, many papers deal with static analysis of the FGM single 2D beams with transverse variation of material properties only. Less attention is paid to longitudinal and lateral variation of material properties. However, the authors did not find papers which consequently deal with all the longitudinal, transversal and lateral variation of material properties by single beams or beam structures built of such FGM.

The presented contribution is the continuation of our previous work dealing with the analysis of beam structures made of planar varying FGM. This approach is extended to spatial variation of material properties and spatial FGM beam structures. Effect of the axial and shear forces (transversal and lateral) and spatial Winkler elastic foundations (except the torsional foundation) are included, as well. The biaxial bending and uniform torsion are considered as well. Homogenization of the spatial varying material properties in the real FGM beam and the calculation of effective parameters are done by the multilayer method (MLM) [43]. If only transversal and lateral variations of material properties are considered in the real FGM beam, longitudinally constant effective material properties arise from the homogenization. This method can also be used in the homogenization of multilayer beams with discontinuous variation of material properties in transversal and lateral direction. Numerical experiments are performed to calculate the elastostatic response of chosen spatial FGM beam structures with rectangular and hollow cross-sections with symmetrically lateral and transversal variations of material properties. The continuous spatial variation of material properties in three directions is considered in the last example, as well. The solution results are discussed and compared to

those obtained by means of very fine 3D – solid and beam finite element mesh of the commercial code.

## 2 Main equations of the 3D beam finite element

Let us consider a 3D straight finite beam element (Timoshenko beam theory and Saint-Venant torsion theory) of doubly symmetric cross-section – Figure 1. The warping effect by non-uniform torsion will be considered in our future work. The nodal degrees of freedom at node  $i$  are: the displacements  $u_i, v_i, w_i$  in the local axis direction  $x, y, z$ , and the cross-sectional area rotations –  $\varphi_{x,i}, \varphi_{y,i}, \varphi_{z,i}$ . The degrees of freedom at the node  $j$  are denoted in a similar manner. The internal forces at node  $i$  are: the axial force  $N_i$ , the transversal forces  $R_{y,i}$  and  $R_{z,i}$ , the bending moments  $M_{y,i}$  and  $M_{z,i}$ , and the torsion moment  $M_{x,i}$ . The first derivative with respect to  $x$  of the relevant variable is denoted with an apostrophe “’”.

Furthermore,  $n_x = n_x(x)$  is the axial force distribution,  $q_z = q_z(x)$  and  $q_y = q_y(x)$  are the transversal and lateral force distributions,  $m_x = m_x(x)$ ,  $m_y = m_y(x)$  and  $m_z = m_z(x)$  are the distributed moments,  $A$  is the cross-sectional area,  $I_y$  and  $I_z$  are the second area moments,  $I_p = I_y + I_z$  is the polar area moment,  $k_x = k_x(x)$ ,  $k_y = k_y(x)$ ,  $k_z = k_z(x)$ ,  $\bar{k}_y = \bar{k}_y(x)$ ,  $\bar{k}_z = \bar{k}_z(x)$  are the elastic foundation modules (the torsional elastic foundation is not considered). The effective homogenized and longitudinally varying stiffness reads:  $EA = E_L^{NH}(x)A$  is the axial stiffness ( $E_L^{NH}(x) \equiv E_L^{NH}$  is the effective elasticity modulus for axial loading),  $EI_y = E_L^{MyH}(x)I_y$  is the flexural stiffness about the  $y$ -axis ( $E_L^{MyH}(x) \equiv E_L^{MyH}$  is the effective elasticity modulus for bending about axis  $y$ ),  $EI_z = E_L^{MzH}(x)I_z$  is the flexural stiffness about the axis  $z$ , ( $E_L^{MzH}(x) \equiv E_L^{MzH}$  is the effective elasticity modulus for bending about axis  $z$ ),  $G\bar{A}_y = G_{Ly}^H(x)k_y^{sm}A$  is the reduced shear stiffness in  $y$  – direction ( $G_{Ly}^H(x) \equiv G_{Ly}^H$  is the effective shear modulus and  $k_y^{sm}$  is the average shear correction factor in  $y$  – direction),  $G\bar{A}_z = G_{Lz}^H(x)k_z^{sm}A$  is the reduced shear stiffness in  $z$  – direction ( $G_{Lz}^H(x) \equiv G_{Lz}^H$  is the effective shear modulus and  $k_z^{sm}$  is the average shear correction factor in  $z$  – direction),  $G_L^{MxH}(x)I_T$  is the effective torsional stiffness ( $G_L^{MxH}(x) = G_L^{MxH}$  is the torsional elasticity modulus and  $I_T$  is the torsion constant).

For establishing of the FGM 3D beam finite element equation we use the following differential equations for axial, transversal, lateral and torsional loading (according the Figure 1).

### 2.1 Axial tension – compression

By combination of the main equations for the axial loading of the FGM beam

$$N' = n_x + k_x u, \quad (1)$$

$$u' = \frac{N}{EA}, \quad (2)$$

we get the differential equation with non-constant polynomial coefficients

$$\eta_{2u} u'' + \eta_{1u} u' + \eta_{0u} u = n_x, \quad (3)$$

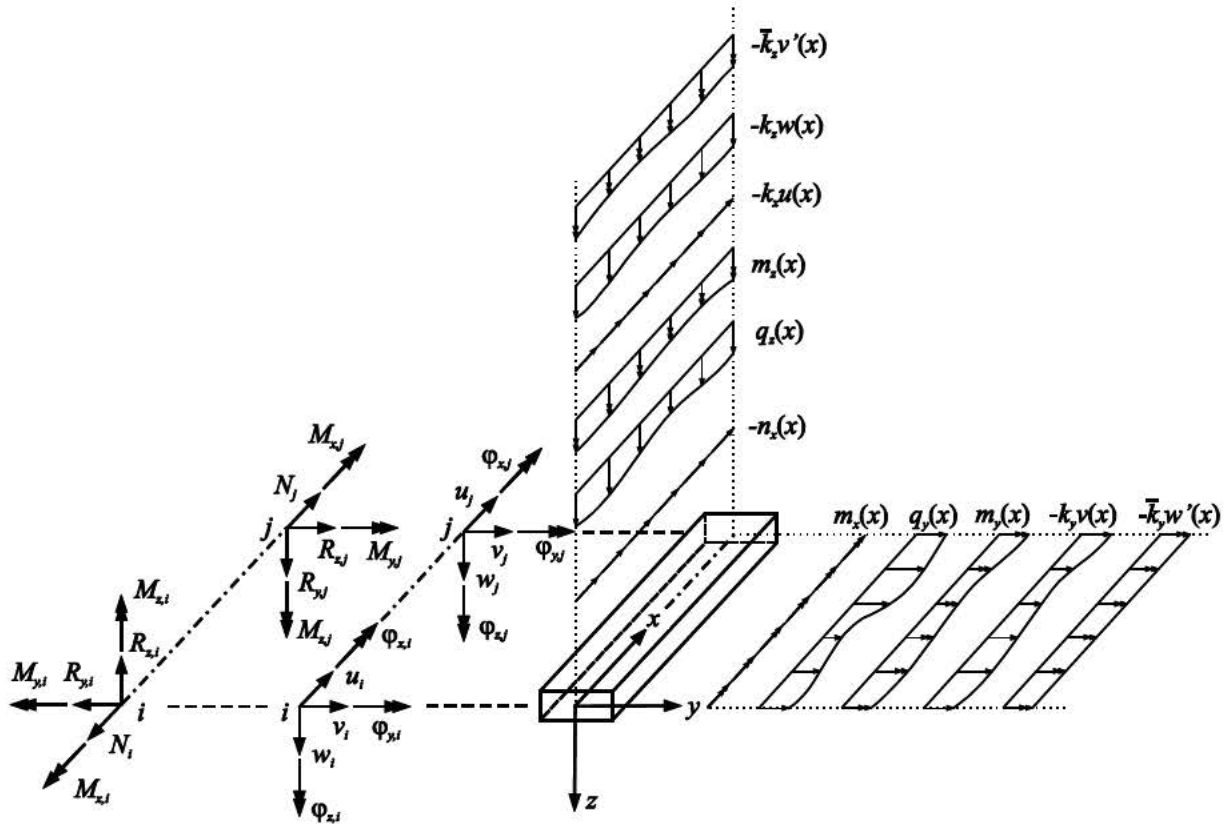


Figure 1: The local internal variables and loads.

with  $\eta_{2u} = EA$ ,  $\eta_{1u} = E'A$ ,  $\eta_{0u} = -k_x$ ,  $N'$  denotes the first derivative of  $N$ ;  $u = u(x)$  is the axial displacement and  $u' = u'(x)$  corresponds to its first derivative and  $u'' = u''(x)$  is its second derivative;  $EA = E_L^{NH}(x)A$  is the homogenized beam stiffness in axial direction and  $E'$  is the first derivative of  $E_L^{NH}(x)$ .

The homogeneous solution of equation (3) can be expressed by the polynomial transfer functions  $\bar{b}_{jN} = \bar{b}_{jN}(x)$ , ( $j \in \{0,1\}$ ) for axial loading (these depend on the axial stiffness variation) [44, 45]:

$$\begin{bmatrix} u(x) \\ u'(x) \end{bmatrix} = \begin{bmatrix} \bar{b}_{0N} & \bar{b}_{1N} \\ \bar{b}'_{0N} & \bar{b}'_{1N} \end{bmatrix} \cdot \begin{bmatrix} u_i \\ u'_i \end{bmatrix}. \quad (4)$$

Here,  $u_i$  is the axial displacement and  $u'_i$  is the value of its first derivative at node  $i$ .

If the  $u'(x)$  and  $u'_i$  are replaced with the constitutive equation  $u' = \frac{N}{EA}$  and  $u'_i = \frac{N_i}{E_i A}$ , we get:

$$\begin{bmatrix} u(x) \\ N(x) \end{bmatrix} = \begin{bmatrix} \bar{b}_{0N} & \frac{\bar{b}_{1N}}{E_i A} \\ EA \bar{b}'_{0N} & \frac{EA}{E_i A} \bar{b}'_{1N} \end{bmatrix} \cdot \begin{bmatrix} u_i \\ N_i \end{bmatrix}, \quad (5)$$

where  $E_i$  is the initial value of the homogenized elasticity modulus  $E_L^{NH}(x)$  at node  $i$ . By setting  $x = L$  in (5) the dependence of the nodal variables at node  $j$  on the nodal variables at node  $i$  are obtained. By appropriate mathematical operations the local finite element equation for axial loading is obtained

$$\begin{bmatrix} N_i \\ N_j \end{bmatrix} = \begin{bmatrix} K_{1,1} & K_{1,7} \\ K_{7,1} & K_{7,7} \end{bmatrix} \begin{bmatrix} u_i \\ u_j \end{bmatrix}, \quad (6)$$

with the local stiffness matrix terms:  $K_{1,1} = \frac{\left[ \bar{b}_{0N} \right]_{x=L}}{\left[ \bar{b}_{1N} \right]_{x=L}} E_{Li}^{NH} A$ ,  $K_{1,7} = K_{7,1} = -\frac{E_{Li}^{NH} A}{\left[ \bar{b}_{1N} \right]_{x=L}}$  and

$K_{7,7} = \frac{\left[ \bar{b}'_{1N} \right]_{x=L}}{\left[ \bar{b}_{1N} \right]_{x=L}} E_{Lj}^{NH} A$ . The variables  $E_{Li}^{NH}$  and  $E_{Lj}^{NH}$  denote the values of the homogenized

elasticity modulus at point  $i$  and  $j$ . Values of the polynomial transfer functions for  $x = L$  are called transfer constants for axial loading, which can be calculated analytically or by simple numerical algorithm [45]. Indices in the stiffness matrix  $K$  are deliberately numbered in order to indicate the position of members of the local axial stiffness matrix in the local matrix of 3D beam finite element (its dimension is  $12 \times 12$ ), which will be established later.

## 2.2 Flexural loading about the $y$ and $z$ axis

The differential equation of 4th order with non-constant coefficients of the homogenized FGM beam flexural deformation (about the  $y$ -axis) (Figure 1) has the form [41],

$$\eta_{4w} w'''' + \eta_{3w} w''' + \eta_{2w} w'' + \eta_{1w} w' + \eta_{0w} w = m_y. \quad (7)$$

Here  $w = w(x)$  is the deflection curve in the  $x - z$  plane. Its derivatives with respect to  $x$  are denoted by an apostrophe.

Derivation of the non-constant coefficients  $\eta_{0w}$  to  $\eta_{4w}$  and appropriated parameters of the differential equation (7) from the main coupled equations (8) and (9) of the 2<sup>nd</sup> order beam theory (including the shear and axial force effects) using the relation between the transversal and shear force (10) is described in [40], [41] and [42] in detail.

$$R'_z = -q_z + k_z w, \quad M'_y = Q_z + m_y, \quad (8)$$

$$\varphi'_y = -\frac{M_y}{EI_y} - \kappa_y^e \Rightarrow M_y = -EI_y \varphi'_y - EI_y \kappa_y^e, \quad w' = \varphi_y + \frac{Q_z}{GA_z} \Rightarrow Q_z = G\bar{A}_z w' - G\bar{A}_z \varphi_y, \quad (9)$$

$$Q_z = -(\bar{k}_z + N'' ) w' + R_z. \quad (10)$$

Here,  $q_z$  is the distributed transversal load;  $m_y$  is the distributed bending moment;  $\kappa_y^e$  is the applied beam curvature;  $k_z$  is the modulus of elastic Winkler foundation;  $R_z$  is the transversal force;  $Q_z$  is the shear force;  $M_y$  is the bending moment;  $\varphi_y$  is the angle of cross-section rotation;  $w$  is the beam deflection;  $EI_y$  is the bending stiffness and  $G\bar{A}_z$  is the reduced shear stiffness of the homogenized FGM beam.  $N'' \equiv N$  is the resultant axial force of the 2<sup>nd</sup> order beam theory. Finally,  $\bar{k}_y$  is the elastic foundation modulus for flexural beam rotation. We assume that all the above quantities are the polynomial functions of  $x$ .

If the variation of the beam parameters is polynomial, the homogeneous solution of the differential equation (7) based on the transfer functions [44] can be written as,

$$\begin{bmatrix} w(x) \\ w'(x) \\ w''(x) \\ w'''(x) \end{bmatrix} = \begin{bmatrix} b_{0w} & b_{1w} & b_{2w} & b_{3w} \\ b'_{0w} & b'_{1w} & b'_{2w} & b'_{3w} \\ b''_{0w} & b''_{1w} & b''_{2w} & b''_{3w} \\ b'''_{0w} & b'''_{1w} & b'''_{2w} & b'''_{3w} \end{bmatrix} \cdot \begin{bmatrix} w_i \\ w'_i \\ w''_i \\ w'''_i \end{bmatrix}. \quad (11)$$

There,  $b_{jw}, b'_{jw}, b''_{jw}$  and  $b'''_{jw}$ , ( $j \in \langle 0,3 \rangle$ ) are the solution functions (transfer functions for flexural deformation (in the  $z$ -axis)) of the differential equation (7). Those depend on the variation of the homogenized bending and shear stiffness of the homogenized beam. The dependence of the  $w' = w'(x)$ ,  $w'' = w''(x)$  and  $w''' = w'''(x)$  on the  $\varphi_y = \varphi_y(x)$ ,  $M_y = M_y(x)$  and  $R_z = R_z(x)$  is described in [40], from which the transfer matrix expression is obtained

$$\begin{bmatrix} w(x) \\ \varphi_y(x) \\ M_y(x) \\ R_z(x) \end{bmatrix} = \begin{bmatrix} A_{1,1} & A_{1,2} & A_{1,3} & A_{1,4} \\ A_{2,1} & A_{2,2} & A_{2,3} & A_{2,4} \\ A_{3,1} & A_{3,2} & A_{3,3} & A_{3,4} \\ A_{4,1} & A_{4,2} & A_{4,3} & A_{4,4} \end{bmatrix} \cdot \begin{bmatrix} w_i \\ \varphi_{y,i} \\ M_{y,i} \\ R_{z,i} \end{bmatrix}. \quad (12)$$

The kinematical and kinetic variables at node  $i$  are denoted by index  $i$  in (12). By setting  $x = L$  in (12) the dependence of the nodal variables at node  $j$  on the nodal variables at node  $i$  will be obtained.

By appropriate mathematical operations the local finite element equation for bending in the  $x - z$  plane is obtained:

$$\begin{bmatrix} R_{z,i} \\ M_{y,i} \\ R_{z,j} \\ M_{y,j} \end{bmatrix} = \begin{bmatrix} K_{3,3} & K_{3,6} & K_{3,9} & K_{3,12} \\ K_{5,2} & K_{5,5} & K_{5,8} & K_{5,11} \\ K_{9,3} & K_{9,6} & K_{9,9} & K_{9,12} \\ K_{11,2} & K_{11,5} & K_{11,8} & K_{11,11} \end{bmatrix} \cdot \begin{bmatrix} w_i \\ \varphi_{y,i} \\ w_j \\ \varphi_{y,j} \end{bmatrix}. \quad (13)$$

Analogically to the axial loading, the local stiffness matrix terms contain the transfer constants for bending which can be calculated analytically or by the simple numerical algorithm [45]. The stiffness terms of the matrix  $K$  are evaluated numerically, and the indexes are deliberately numbered so as to indicate the position of the terms of the matrix in the local stiffness matrix of the 3D beam finite element, which will be established later.

Differential equation of the 4th order with non-constant coefficients for the homogenized FGM beam flexural deformation (about the  $z$ -axis), (Figure 1), can be derived similarly to the previous case,

$$\eta_{4v} v'''' + \eta_{3v} v'''' + \eta_{2v} v'' + \eta_{1v} v' + \eta_{0v} v = m_z. \quad (14)$$

By appropriate mathematical operations the local finite element equations for flexural deformation (in the  $x - y$  plane) are obtained,

$$\begin{bmatrix} R_{y,i} \\ M_{z,i} \\ R_{y,j} \\ M_{z,j} \end{bmatrix} = \begin{bmatrix} K_{2,2} & K_{2,6} & K_{2,8} & K_{2,12} \\ K_{6,2} & K_{6,6} & K_{6,8} & K_{6,12} \\ K_{8,2} & K_{8,6} & K_{8,8} & K_{8,12} \\ K_{12,2} & K_{12,6} & K_{12,8} & K_{12,12} \end{bmatrix} \cdot \begin{bmatrix} v_i \\ \varphi_{z,i} \\ v_j \\ \varphi_{z,j} \end{bmatrix}. \quad (15)$$

### 2.3 Uniform torsion

The differential equations of uniform torsion of the FGM beam are formulated according the Figure 1 and have a form,

$$M'_x = m_x, \quad (16)$$

$$\varphi'_x = \frac{M_x}{G_L^{M_x H} I_T}. \quad (17)$$

There,  $I_T$  is the torsion constant ( $I_T = I_p$  for the circular cross-section and  $I_p$  is the polar area moment);  $\varphi_x = \varphi_x(x)$  is the torsion angle of rotation;  $\varphi'_x$  is a first derivative of the torsion angle. An elastic foundation for torsion is not considered.

By a combination of equations (16) and (17) and after some mathematical manipulations the differential equation for uniform torsional loading has been obtained

$$\eta_{2T} \varphi_x'' + \eta_{1T} \varphi_x' = m_x, \quad (18)$$

with non-constant parameters  $\eta_{1T} = G_L^{M_x H} I_T$ ;  $\eta_{2T} = G_L^{M_x H} I_T$ . According to [44], the homogeneous solution of the differential equation (18) reads:

$$\begin{bmatrix} \varphi_x(x) \\ \varphi'_x(x) \end{bmatrix} = \begin{bmatrix} \bar{b}_{0T} & \bar{b}_{1T} \\ \bar{b}'_{0T} & \bar{b}'_{1T} \end{bmatrix} \cdot \begin{bmatrix} \varphi_{x,i} \\ \varphi'_{x,i} \end{bmatrix} \quad (19)$$

In equation (19), the  $\bar{b}_{jT}$  and  $\bar{b}'_{jT}$ ,  $j \in \langle 0,1 \rangle$ , are the transfer functions (of  $x$ ) and their first derivatives, respectively. Those are the solution functions of the differential equation (18). The transfer functions depend on the longitudinal variation of the torsional shear modulus. By inserting (16) and (17) into (19) the transfer matrix relations (20) for uniform torsion is obtained after some mathematical manipulations,

$$\begin{bmatrix} \varphi_x(x) \\ M_x(x) \end{bmatrix} = \begin{bmatrix} \bar{b}_{0T} & \frac{\bar{b}_{1T}}{G_{Li}^{M_x H} I_T} \\ G_L^{M_x H} I_T \bar{b}'_{0T} & \frac{G_L^{M_x H} I_T \bar{b}'_{1T}}{G_{Li}^{M_x H} I_T} \end{bmatrix} \cdot \begin{bmatrix} \varphi_{x,i} \\ M_{x,i} \end{bmatrix}. \quad (20)$$

By setting  $x = L$  in (20) a dependence of the state variables at point  $j$  on the state variables at initial point  $i$  for modal analysis reads:

$$\begin{bmatrix} \varphi_{x,j} \\ M_{x,j} \end{bmatrix} = \begin{bmatrix} [\bar{b}_{0T}]_{x=L} & \frac{[\bar{b}_{1T}]_{x=L}}{G_{Li}^{M_x H} I_T} \\ G_{Lj}^{M_x H} I_T [\bar{b}'_{0T}]_{x=L} & \frac{G_{Lj}^{M_x H} I_T [\bar{b}'_{1T}]_{x=L}}{G_{Li}^{M_x H} I_T} \end{bmatrix} \cdot \begin{bmatrix} \varphi_{x,i} \\ M_{x,i} \end{bmatrix}. \quad (21)$$

By simple mathematical manipulations we get the local finite element equation for uniform torsion:

$$\begin{bmatrix} M_{x,i} \\ M_{x,j} \end{bmatrix} = \begin{bmatrix} K_{4,4} & K_{4,10} \\ K_{10,4} & K_{10,10} \end{bmatrix} \cdot \begin{bmatrix} \varphi_{x,i} \\ \varphi_{x,j} \end{bmatrix}, \quad (22)$$

with the finite element stiffness matrix terms:  $K_{4,4} = \frac{[\bar{b}_{0T}]_{x=L}}{[\bar{b}_{1T}]_{x=L}} G_{Li}^{M_x H} I_T$ ,  $K_{4,10} = -\frac{G_{Li}^{M_x H} I_T}{[\bar{b}_{1T}]_{x=L}}$ ,

$K_{10,4} = K_{4,10}$ ,  $K_{10,10} = \frac{[\bar{b}'_{1T}]_{x=L}}{[\bar{b}_{1T}]_{x=L}} G_{Lj}^{M_x H} I_T$ . The transfer constants  $[\bar{b}_{jT}]_{x=L}$  and  $[\bar{b}'_{jT}]_{x=L}$ ,  $j \in \langle 0,1 \rangle$ ,

can be calculated with a simple numerical algorithm [44, 45]. The  $G_{Li}^{M,H}$  and  $G_{Lj}^{M,H}$  are the values of the homogenized torsional shear modulus at point  $i$  and  $j$ .

#### 2.4 Local 3D FGM finite beam element equation

The local finite element equation of the 3D – FGM beam is obtained by superposition of the axial (6), flexural transversal (13), flexural lateral (15) and torsional (22) stiffness equations, and it reads,

$$\begin{bmatrix} N_i \\ R_{y,i} \\ R_{z,i} \\ M_{x,i} \\ M_{y,i} \\ M_{z,i} \\ N_j \\ R_{y,j} \\ R_{z,j} \\ M_{x,j} \\ M_{y,j} \\ M_{z,j} \end{bmatrix} = \begin{bmatrix} K_{1,1} & 0 & 0 & 0 & 0 & 0 & K_{1,7} & 0 & 0 & 0 & 0 & 0 \\ & K_{2,2} & 0 & 0 & 0 & K_{2,6} & 0 & K_{2,8} & 0 & 0 & 0 & K_{2,12} \\ & & K_{3,3} & 0 & K_{3,5} & 0 & 0 & 0 & K_{3,9} & 0 & K_{3,11} & 0 \\ & & & K_{4,4} & 0 & 0 & 0 & 0 & 0 & K_{4,10} & 0 & 0 \\ S & & & & K_{5,5} & 0 & 0 & 0 & K_{5,9} & 0 & K_{5,11} & 0 \\ & Y & & & & K_{6,6} & 0 & K_{6,8} & 0 & 0 & 0 & K_{6,12} \\ & & M & & & & K_{7,7} & 0 & 0 & 0 & 0 & 0 \\ & & & M & & & & K_{8,8} & 0 & 0 & 0 & K_{8,12} \\ & & & & E & & & & K_{9,9} & 0 & K_{9,11} & 0 \\ & & & & & T & & & & K_{10,10} & 0 & 0 \\ & & & & & & R & & & & K_{11,11} & 0 \\ & & & & & & & Y & & & & K_{12,12} \end{bmatrix} \cdot \begin{bmatrix} u_i \\ v_i \\ w_i \\ \varphi_{x,i} \\ \varphi_{y,i} \\ \varphi_{z,i} \\ u_j \\ v_j \\ w_j \\ \varphi_{x,j} \\ \varphi_{y,j} \\ \varphi_{z,j} \end{bmatrix} \quad (23)$$

In (23), the bending terms of the stiffness matrix  $K$  consist of linear and linearized geometric non-linear stiffness terms. The linearized terms consider the axial force  $N''$  influence only (according to the assumptions of the second order beam theory). The global stiffness matrix of the beam finite element and the beam structure can be established by a conventional method. Algorithm for establishing of the local and global stiffness matrices as well as the whole procedure for the global and local nodal displacements calculation we have coded in the MATHEMATICA [46] software environment, by which the numerical experiments were done. The secondary variables (internal forces and moments) on the real beams are then calculated by means of the transfer relations (5), (12), (20). Again, the normal and shear stress can be calculated [54] on the real beams. In order to show the accuracy and effectiveness of proposed 3D FGM finite beam element, numerical experiments are made concerning the elastic-static analyses of the single beams and beam structures made of spatially varying FGM properties.

### 3 Homogenization of spatial varying material properties for the 3D beam applications by the multilayering method

One important goal of mechanics of heterogeneous materials is to derive their effective properties from the knowledge of the constitutive laws and complex micro-structural behavior of their components. Microscopic modeling expresses the relation between the characteristics of the components (constituents) and the average (effective) properties of the composite. In the case of FGM beam, it is the relation between the material properties of the beam components and the effective material properties of the homogenized beam.

The methods, based on the homogenization theory (e.g. the mixture rules [47], [48]; self-consistent methods [49]), have been designed and successfully applied to determine the effective material properties of heterogeneous materials from the corresponding material behavior of the constituents (and of the interfaces between them) and from the geometrical

arrangement of the phases. In this context, the microstructure of the material under consideration is basically taken into account by a representative volume element (RVE).

Mixture rules are one of the methods for micromechanical modeling of heterogeneous materials. Extended mixture rules [50] are based on the assumption that the constituents volume fractions (formally only denoted here as fibres –  $f$  and matrix –  $m$ ) continuously vary as polynomial functions,  $v_f(x, y, z)$  and  $v_m(x, y, z)$ . The condition  $v_f(x, y, z) + v_m(x, y, z) = 1$  has to be fulfilled. The appropriated material property distribution in the real FGM beam (Figure 2a) then reads

$$p(x, y, z) = v_f(x, y, z)p_f(x, y, z) + v_m(x, y, z)p_m(x, y, z) \quad (24)$$

Here,  $p_f(x, y, z)$  and  $p_m(x, y, z)$  are the spatial distributions of material properties of the FGM constituents. The extended mixture rule (24) can be analogically used for FGM material made of more than two constituents. The assumption of a polynomial variation of the constituent's volume fractions and material properties enables an easier establishing of the main appropriated field equations and allows the modeling of many common realizable variations. In literature and in practical applications, mostly the one directional variation of the FGM properties is considered. There, an exponential law for transversal variation of the constituents volume fractions is often presented, e.g. in [51], [52], [53] and in references therein.

For the FGM beams and shells the transversal variation (continuously or discontinuously, symmetrically or asymmetrically) has been mainly considered. The homogenization of such material properties variation is relatively simple. If the material properties vary only with respect to the longitudinal direction, the homogenization is frequently not needed since there are new FGM beam and link finite elements established that consider such variations in a very accurate and effective way, e.g. in [54], [55]. A more complicated case is, if the material properties vary in three directions - namely in transversal, lateral and longitudinal direction of the FGM real beam and the torsion is included as well.

In this contribution, the homogenization techniques for spatially varying (continuously or discontinuously and symmetrically in transversal and lateral direction, and continuously in longitudinal direction) material properties of FGM beams of selected doubly-symmetric cross-sections are presented. The expressions are proposed for the derivation of effective elasticity modulus for axial loading, the transversal and lateral bending, the shear modulus for transversal and lateral shear and for uniform torsion by the extended mixture rules (EMR) and the multilayer method (MLM). The case of non-uniform torsion will be considered in our future work.

Let us consider a two noded 3D straight beam element with double symmetric cross-sectional area  $A$  (Figure 2). The composite material of this beam arises from mixing two components. The continuous polynomial spatial variation of the elasticity moduli and mass density can be caused by continuous polynomial spatial variation of both the volume fraction ( $v_f(x, y, z)$  and  $v_m(x, y, z)$ ) and material properties of the FGM constituents ( $p_f(x, y, z)$  and  $p_m(x, y, z)$ ).

In our case the elasticity modulus  $E(x, y, z)$ , the Poisson ratio for the real beam have been calculated by expression (24). The FGM shear modulus can be calculated by expression:

$$G(x, y, z) = \frac{E(x, y, z)}{2(1 + \nu(x, y, z))}. \quad (25)$$

If the constituents Poisson's ratio are approximately of the same value and the constituent volume fractions variation is not strong, then the FGM shear modulus can be calculated using a simplification [42]:

$$G(x, y, z) = \frac{E(x, y, z)}{\xi}, \quad (26)$$

where  $\xi$  is an average value of the function  $\xi(x, y, z) = 2(1 + \nu(x, y, z))$

$$\xi = \frac{1}{L} \int_0^L \left( \frac{1}{A} \int_{(A)} \xi(x, y, z) dA \right) dx. \quad (27)$$

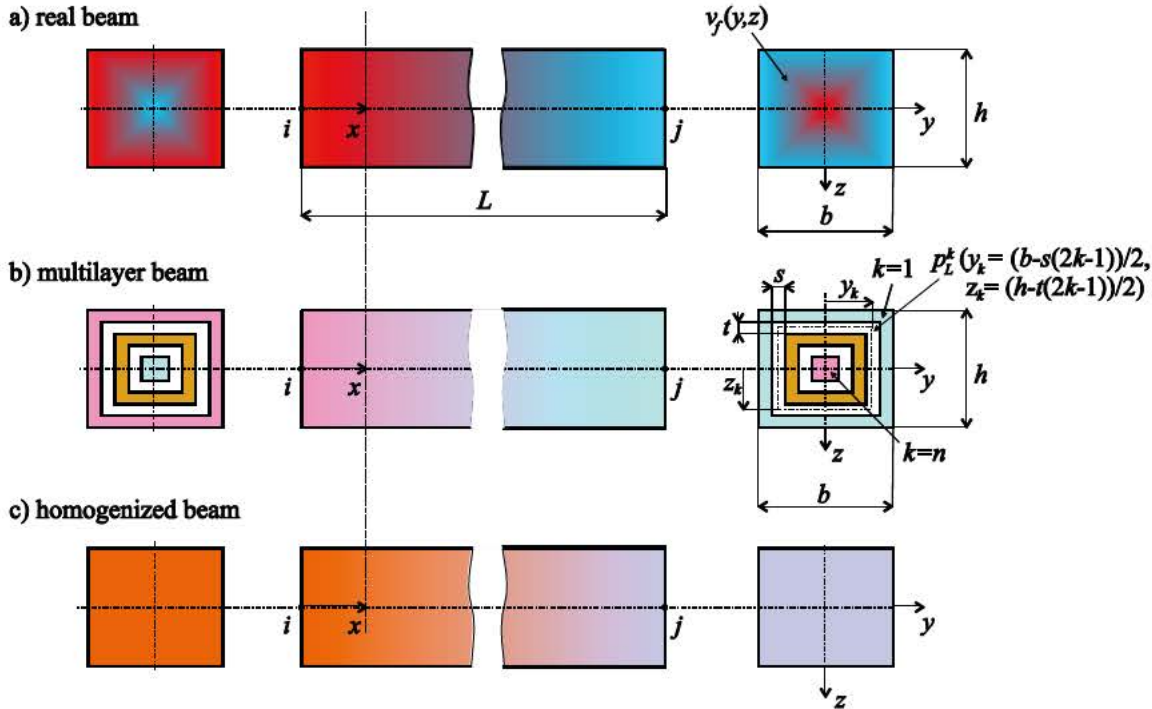


Figure 2: FGM beam with rectangular cross-section.

Homogenization of the spatially varying material properties (the reference volume is the volume of the whole beam) are done in two steps. In the first step, the real beam (Figure 2a) is transformed into a multilayer beam (Figure 2b). Material properties of the layers are calculated with the EMR [56]. We assume that each layer cross-section at position  $x$  has constant material properties. They are calculated as an average value from their values at the boundaries of the respective layer cross-section. Polynomial variation of these properties appears in the longitudinal direction of the layer. Sufficient accuracy of the proposed substitution of the continuous transversal and lateral variation of material properties by the layer-wise constant distribution of material properties is reached if the division to layers is fine enough. In the second step, the effective longitudinal material properties of the homogenized beam are derived using the MLM [57]. These homogenized material properties are constant through the beam's height and depth but they vary continuously along the longitudinal beam axis. Accordingly, the beam finite element equation are established for the homogenized beam (Figure 2c) in order to calculate the primary beam unknowns – the displacements and internal forces and critical buckling force in our case. The stress has to be calculated on the real beam.

The homogenized elasticity moduli for: tension-compression -  $E_L^{NH}(x)$ , bending about axis  $y$  -  $E_L^{MyH}(x)$ , bending about axis  $z$  -  $E_L^{MzH}(x)$ , shear in  $y$  direction -  $G_{Ly}^H(x)$ , shear in  $z$  direction -  $G_{Lz}^H(x)$ , and torsion  $G_L^{MxH}(x)$  can be calculated, respectively:

$$E_L^{NH}(x) = \frac{\sum_{k=1}^n E_k(x) A_k}{A}, \quad E_L^{M_y H}(x) = \frac{\sum_{k=1}^n E_k(x) I_{y,k}}{I_y}, \quad E_L^{M_z H}(x) = \frac{\sum_{k=1}^n E_k(x) I_{z,k}}{I_z}, \quad (28)$$

$$G_{L_y}^H(x) = \frac{\sum_{k=1}^n k_{y,k}^{sm} G_k(x) A_k}{k_y^{sm} A}, \quad G_{L_z}^H(x) = \frac{\sum_{k=1}^n k_{z,k}^{sm} G_k(x) A_k}{k_z^{sm} A}, \quad G_L^{M_x H}(x) = \frac{\sum_{k=1}^n G_k(x) I_{T,k}}{I_T}. \quad (29)$$

Here,  $A_k$  is the cross-sections area,  $E_k(x)$  is the elasticity modulus,  $I_{y,k}$  and  $I_{z,k}$  are the second moments of area,  $G_k(x)$  is the shear modulus,  $I_{T,k}$  is the torsion constant of the  $k$ th layer, respectively. Again,  $k_{y,k}^{sm}$  and  $k_{z,k}^{sm}$  and  $k_y^{sm}$  and  $k_z^{sm}$  are the average shear correction factors [58].

Exact expressions for homogenization of spatial varying (continuously or discontinuously and symmetrically in transversal and lateral direction, and continuously in longitudinal direction) material properties for the FGM beams depend of the cross-section shape. In the following chapters, we present derivation of the corresponding expressions for rectangular cross-section. By similar way the effective material properties can be calculated for the hollow, circular and ring cross-sections [59].

### 3.1 Rectangular cross-section

A straight beam of rectangular cross-sectional area  $A = bh$  (Figure 2) is made of a FGM which properties vary in the  $y$  and  $z$  direction continuously and symmetrically according the main inertial planes:  $x - y$  and  $x - z$ , and continuously in longitudinal beam direction  $x$ .

Further,  $I_y = \frac{bh^3}{12}$  and  $I_z = \frac{hb^3}{12}$  are the second moments of area,  $I_p = I_y + I_z$  is the cross-sectional area polar moment,  $\bar{A}_y = k_y^{sm} A$  and  $\bar{A}_z = k_z^{sm} A$  are the reduced cross-sectional areas – by the average shear correction factors  $k_y^{sm}$  and  $k_z^{sm}$  [20], and  $I_T = \alpha hb^3$  is the torsion constant ( $\alpha = f(h/b)$  is the rectangular cross-section parameter). According to (24) the real material properties are the elasticity modulus  $E(x, y, z)$ , the Poisson's ratio  $\nu(x, y, z)$  and the shear modulus  $G(x, y, z) = E(x, y, z) / (2(1 + \nu(x, y, z)))$ . For the homogenization of spatially varying material properties the rectangular cross-sectional area is divided into  $n$  parts, where  $t = h/2n$  refers to the flange thickness and  $s = b/2n$  denotes the web thickness (Figure 2b). Again,  $A_n = 2s2t$  and the hollow area of the  $k$ th part ( $k \in \langle 1, n-1 \rangle$ ) is  $A_k = 2t(b - s(2k - 1)) + 2s(h - t(2k - 1))$ . The second moments of area of the  $n$ th part are:  $I_{y,n} = 2s(2t)^3 / 12$  and  $I_{z,n} = 2t(2s)^3 / 12$ . The second moments of area of the  $k$ th part are:

$$I_{y,k} = (b - s(2k - 2))(h - t(2k - 2))^3 / 12 - (b - 2ks)(h - 2kt)^3 / 12,$$

$$I_{z,k} = (b - s(2k - 2))^3 (h - t(2k - 2)) / 12 - (b - 2ks)^3 (h - 2kt) / 12.$$

The torsion constant of the  $n$ th rectangular part is:  $I_{T,n} = \alpha_n 2s(2t)^3$ . The torsion constant of the  $k$ th hollow part ( $k \in \langle 1, n-1 \rangle$ ) is:

$$I_{T,k} = \frac{2(b - s(2k - 1))^2 (h - t(2k - 1))^2}{\frac{(b - s(2k - 1))}{t} + \frac{(h - t(2k - 1))}{s}}. \quad (30)$$

We assume, that the considered material property is constant in all parts  $k \in \langle 1, n-1 \rangle$  of the cross sectional area  $A$  and it varies in the  $x$ -axis direction only:

$$p_k(x) = [p(x, y, z)]_{z=z_k}^{y=y_k}. \quad (31)$$

There, according to Figure 2,  $y_k = \frac{b-s(2k-1)}{2}$  and  $z_k = \frac{h-t(2k-1)}{2}$ . For the  $n$ th part  $y_n = t/2$  and  $z_n = s/2$ .

The effective homogenized material properties, like the elasticity modules, have been calculated under the assumption, that the relevant stiffness of the homogenized beam is equal to the stiffness of the real beam virtually divided in the rectangular and hollow parts. So we get the effective elasticity modulus for axial loading

$$E_L^{NH}(x) = \frac{E_n(x)A_n + \sum_{k=1}^{n-1} E_k(x)A_k}{A}, \quad (32)$$

with  $E_n(x) = [E(x, y, z)]_{z=z_n}^{y=y_n}$  and  $E_k(x) = [E(x, y, z)]_{z=z_k}^{y=y_k}$ , and the effective elasticity modules for bending about the  $y$  and  $z$  axis

$$E_L^{M_yH}(x) = \frac{E_n(x)I_{y,n} + \sum_{k=1}^{n-1} E_k(x)I_{y,k}}{I_y}, \quad E_L^{M_zH}(x) = \frac{E_n(x)I_{z,n} + \sum_{k=1}^{n-1} E_k(x)I_{z,k}}{I_z}. \quad (33)$$

The effective elasticity modulus for uniform torsion reads,

$$G_L^{M_xH}(x) = \frac{G_n(x)I_{T,n} + \sum_{k=1}^{n-1} G_k(x)I_{T,k}}{I_T}, \quad (34)$$

with  $G_n(x) = [G(x, y, z)]_{z=z_n}^{y=y_n}$  and  $G_k(x) = [G(x, y, z)]_{z=z_k}^{y=y_k}$ . The effective shear modulus in  $y$  direction is given by

$$G_{Ly}^H(x) = \frac{k_{y,n}^{sm} G_n(x)A_n + \sum_{k=1}^{n-1} k_{y,k}^{sm} G_k(x)A_k}{k_y^{sm} A}, \quad (35)$$

with the average shear correction factors,  $k_y^{sm}$  for whole rectangular cross-section,  $k_{y,n}^{sm}$  for  $n$ th part and  $k_{y,k}^{sm}$  for  $k$ th part.

The shear modulus in  $z$  direction reads analogically

$$G_{Lz}^H(x) = \frac{k_{z,n}^{sm} G_n(x)A_n + \sum_{k=1}^{n-1} k_{z,k}^{sm} G_k(x)A_k}{k_z^{sm} A}, \quad (36)$$

with the average shear correction factors:  $k_z^{sm}$  for whole rectangular cross-section,  $k_{z,n}^{sm}$  for  $n$ th part and  $k_{z,k}^{sm}$  for  $k$ th part[58].

### 3.2 Hollow cross-section

A straight beam of hollow cross-sectional area  $A = b_1 h_1 - b_n h_n$  (Figure 3) is made of FGM that properties vary in the  $y$  and  $z$  direction continuously and symmetrically according to the main inertial planes,  $x-y$  and  $x-z$ , and continuously in longitudinal beam direction  $x$ .

Further,  $I_y = \frac{b_1 h_1^3}{12} - \frac{b_n h_n^3}{12}$  and  $I_z = \frac{h_1 b_1^3}{12} - \frac{h_n b_n^3}{12}$  are the second moments of area,

$I_p = I_y + I_z$  is the polar moment of area,  $\bar{A}_y = k_y^{sm} A$  and  $\bar{A}_z = k_z^{sm} A$  are the reduced cross-sectional areas – by the average shear correction factors  $k_y^{sm}$  and  $k_z^{sm}$  [50], and

$I_T = \frac{2(h_1 - t)^2 (b_1 - s)^2}{\frac{h_1 - t}{s} + \frac{b_1 - s}{t}}$  is the torsion constant. Here,  $s$  and  $t$  refer to the thicknesses of the

cross-section walls.

For the homogenization of spatially varying material properties the hollow cross-sectional area is divided into  $n$  hollow parts, where  $t_k = (h_1 - h_n)/2n$  is the flange thickness and  $s_k = (b_1 - b_n)/2n$  is the web thickness (Figure 4), respectively. The hollow area of the  $k$ th part ( $k \in \langle 1, n \rangle$ ) is:  $A_k = 2t_k(b_1 - s_k(2k - 1)) + 2s_k(h_1 - t_k(2k - 1))$ . The second moments of area of the  $k$ th part are:  $I_{y,k} = (b_1 - s_k(2k - 2))(h_1 - t_k(2k - 2))^3 / 12 - (b_1 - 2ks_k)(h - 2kt_k)^3 / 12$ ,  $I_{z,k} = (b_1 - s_k(2k - 2))^3 (h_1 - t_k(2k - 2)) / 12 - (b_1 - 2ks_k)^3 (h_1 - 2kt_k) / 12$ .

The polar moment of area of  $k$ th part is  $I_{p,k} = I_{y,k} + I_{z,k}$ .

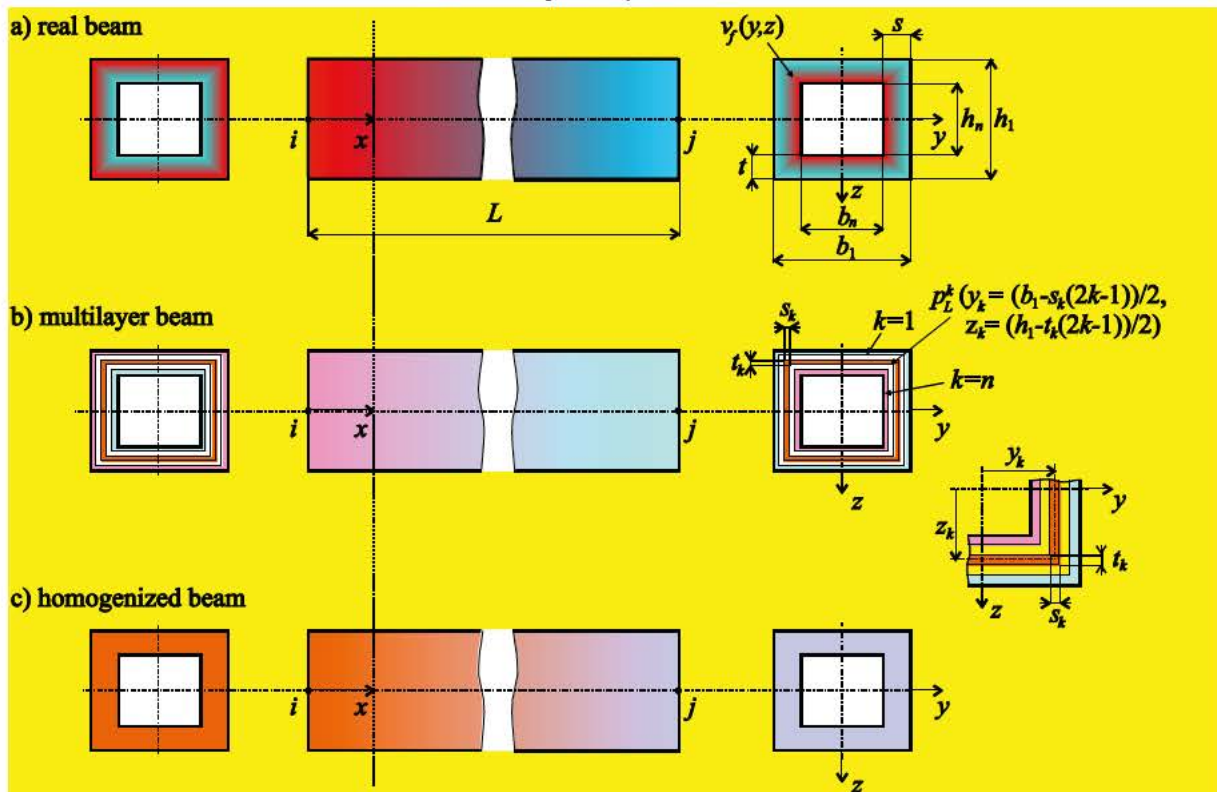


Figure 3: A straight FGM beam of hollow cross-section.

According to (24) the real material properties are:  $E(x, y, z)$  is the elasticity modulus,  $\nu(x, y, z)$  is the Poisson's ratio,  $G(x, y, z) = E(x, y, z) / (2(1 + \nu(x, y, z)))$  is the shear modulus and  $\rho(x, y, z)$  is the mass density:

$$(x \in \langle 0, L \rangle, y \in \langle \pm h_n / 2, \pm h_1 / 2 \rangle, z \in \langle \pm b_n / 2, \pm b_1 / 2 \rangle).$$

The effective homogenized material properties, like the elasticity modulus, are calculated under assumption, that the relevant stiffness of the homogenized beam is equal to the stiffness of the real beam virtually divided on the hollow parts. So we get the effective elasticity modulus for axial loading

$$E_L^{NH}(x) = \frac{\sum_{k=1}^{n-1} E_k(x) A_k}{A}, \quad (37)$$

with  $E_k(x) = [E(x, y, z)]_{z=z_k}^{y=y_k}$  and the effective elasticity modulus for bending about the  $y$  and  $z$  axis,

$$E_L^{M_yH}(x) = \frac{\sum_{k=1}^n E_k(x) I_{y,k}}{I_y}, \quad E_L^{M_zH}(x) = \frac{\sum_{k=1}^n E_k(x) I_{z,k}}{I_z}. \quad (38)$$

The effective elasticity modulus for uniform torsion reads,

$$G_L^{M_xH}(x) = \frac{\sum_{k=1}^n G_k(x) I_{T,k}}{I_T}, \quad (39)$$

with  $G_k(x) = [G(x, y, z)]_{z=z_k}^{y=y_k}$ . The torsion constant of the  $k$ th hollow part ( $k \in \langle 1, n \rangle$ ) can be evaluated as

$$I_{T,k} = \frac{2(b_1 - s_k(2k-1))^2 (h_1 - t_k(2k-1))^2}{\frac{(b_1 - s_k(2k-1))}{t_k} + \frac{(h_1 - t_k(2k-1))}{s_k}}. \quad (40)$$

The effective shear modulus in  $y$  direction is given by,

$$G_{Ly}^H(x) = \frac{\sum_{k=1}^n k_{y,k}^{sm} G_k(x) A_k}{k_y^{sm} A}, \quad (41)$$

with the average shear correction factors:  $k_y^{sm}$  for whole rectangular cross-section and  $k_{y,k}^{sm}$  for  $k$ th part.

The shear modulus in  $z$  direction then reads,

$$G_{Lz}^H(x) = \frac{\sum_{k=1}^n k_{z,k}^{sm} G_k(x) A_k}{k_z^{sm} A}, \quad (42)$$

with the average shear correction factors:  $k_z^{sm}$  for whole rectangular cross-section and  $k_{z,k}^{sm}$  for  $k$ th part.

## 4 Numerical experiments

### 4.1 Example 1 - FGM cantilever beam- rectangular cross-section

The clamped FGM beam has been considered (as shown in Figure 4), which is loaded at its free end by forces  $F_y = F_z = 10\text{ N}$  and  $F_x = -5\text{ kN}$  and by torsion moment  $M_x = 10\text{ Nm}$ . Its rectangular cross-section is constant with height  $h = 0.005\text{ m}$  and width  $b = 0.01\text{ m}$ . The length of the beam is  $L = 0.1\text{ m}$ . The local coordinates system is denoted by the axis  $x, y$ , and  $z$ .

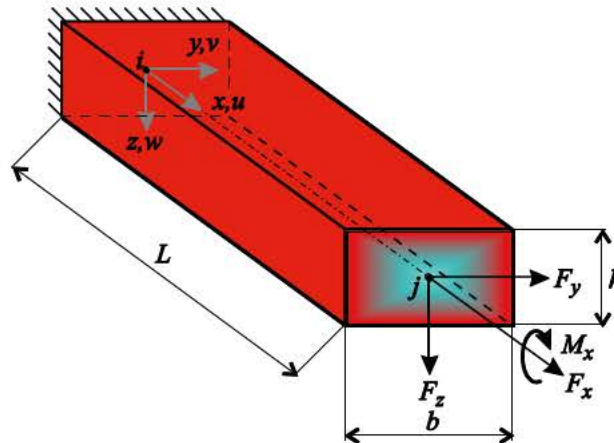


Figure 4: FGM beam with spatial variation of material properties.

Material of the beam consists of two components: Aluminum Al6061-TO – denoted with index  $m$  and Titanium carbide TiC – denoted with index  $f$ . The material properties of the components are assumed to be constant and their values are: Aluminum Al6061-TO – the elasticity modulus  $E_m = 69.0\text{ GPa}$ , the Poisson's ratio  $\nu_m = 0.33$ ; Titanium carbide TiC – the elasticity modulus  $E_f = 480.0\text{ GPa}$ , the Poisson's ratio  $\nu_f = 0.20$ .

The TiC volume fraction varies in the  $y$  and  $z$  direction linearly and symmetrically according to the  $x$ - $y$  and  $x$ - $z$  planes:  $[v_f(y, z)]_{z=0} = 0, [v_f(y, z)]_{z=\pm h/2} = 1$  - the core of the beam is made from pure Al6061-TO and linearly varies to the edges that are made from pure TiC. Constant effective material properties are considered in the local  $x$  – direction of the beam. The average shear correction factors in  $y$  – direction  $k_y^{sm} = 5/6$  and in  $z$  – direction  $k_z^{sm} = 5/6$  have been considered (constant Poisson ratio has been assumed in the example).

Using the EMR and MLM, the homogenized elasticity modules (in [GPa]) for: axial loading -  $E_L^{NH}$ , bending about axis  $y$  -  $E_L^{M_y, H}$  and about axis  $z$  -  $E_L^{M_z, H}$ , shear -  $G_{Ly}^H$  and  $G_{Lz}^H$ , and torsion -  $G_L^{M_x, H}$  have been calculated. The influence of the number of divisions  $n$  to the layers on the homogenized material properties are shown in the Table 1.

Table 1: Homogenized material properties for  $n = 2, 5, 10, 15$  and  $20$  layers

layers $n$	$E_L^{NH}$	$E_L^{M_y, H} = E_L^{M_z, H}$	$G_{Ly}^H = G_{Lz}^H$	$G_L^{M_x, H}$
2	300.19	357.98	121.27	145.10
5	338.62	392.28	137.11	160.59
10	342.11	396.43	138.58	162.23
15	342.64	397.19	138.81	162.52
20	342.80	397.46	138.88	162.62

The FGM beam, clamped at the node  $i$ , has been studied by the elastic-static and buckling analysis. All the calculations were done with our 3D FGM beam finite element (NFE) which we have implemented into the code MATHEMATICA [46]. Additionally, the effect of axial force was considered. It has to be pointed out that the entire structure is discretized using only one herein proposed finite element. The critical buckling force is  $N_{ki}'' = 10.28 \text{ kN}$ . In the elasto-static analysis the axial force (tension and compression)  $N'' \equiv N$  have been chosen as a part of the critical buckling force  $N_{ki}''$ . The effective material properties were used from the last line in the Table 1. The deformations and internal forces and moments are found in the example.

The same problem has been solved using a very fine mesh – 28889 of SOLID186 elements of the FEM program ANSYS [60] (geometric nonlinear). The results of ANSYS as well as the results of the NFE are presented in Tables 2. The average relative difference  $\Delta$  [%] between displacements calculated by our method and the ANSYS solution has been evaluated.

Table 2: Displacements at the free beam end

Displacements [mm], [rad]	NFE $F_x = 0 \text{ N}$	ANSYS $F_x = 0 \text{ N}$	$\Delta$ [%]	NFE $F_x = -5 \text{ kN}$	ANSYS $F_x = -5 \text{ kN}$	$\Delta$ [%]
$u_j$	0	0	---	-0.029230	-0.029385	0.53
$v_j$	0.020349	0.020271	0.38	0.022281	0.022173	0.49
$w_j$	0.080879	0.080645	0.29	0.158012	0.157130	0.56
$\varphi_{x,j}$	0.021533	0.021844	1.42	0.021534	0.021185	1.47
$\varphi_{y,j}$	-0.001211	-0.001206	0.43	-0.000346	-0.000344	0.75
$\varphi_{z,j}$	0.000303	0.000302	0.03	0.002417	0.002410	0.26

As is shown in Table 2, the accuracy of our results is excellent compared to the ANSYS solution.

The Figures 5, 6, 7 and 8 show the total deformation of FGM beam, torsion moment and bending moment about the  $y$  and  $z$  – axis, respectively. The Figures 9 and 10 show the transversal force in  $y$  and  $z$  – axis. The comparison of the bending moments  $M_y(x=0)$ ,  $M_z(x=0)$  and transversal forces  $R_y(x=L)$ ,  $R_z(x=L)$  for the case  $F_x = -5 \text{ kN}$  calculated by our approach and by ANSYS are compared in Table 3.

Table 3: Bending moments and transversal forces

	NFE $F_x = -5 \text{ kN}$	ANSYS $F_x = -5 \text{ kN}$	$\Delta$ [%]
$M_y(x=0)$ [Nm]	-1.781	-1.788	0.39
$M_z(x=0)$ [Nm]	1.123	1.116	0.59
$R_y(x=L)$ [N]	11.811	12.166	2.66
$R_z(x=L)$ [N]	22.102	21.756	1.56

The high efficiency of our method is obvious since our results are evaluated using only one finite beam element compared to the large number of 41924 elements used in the continuum mesh.

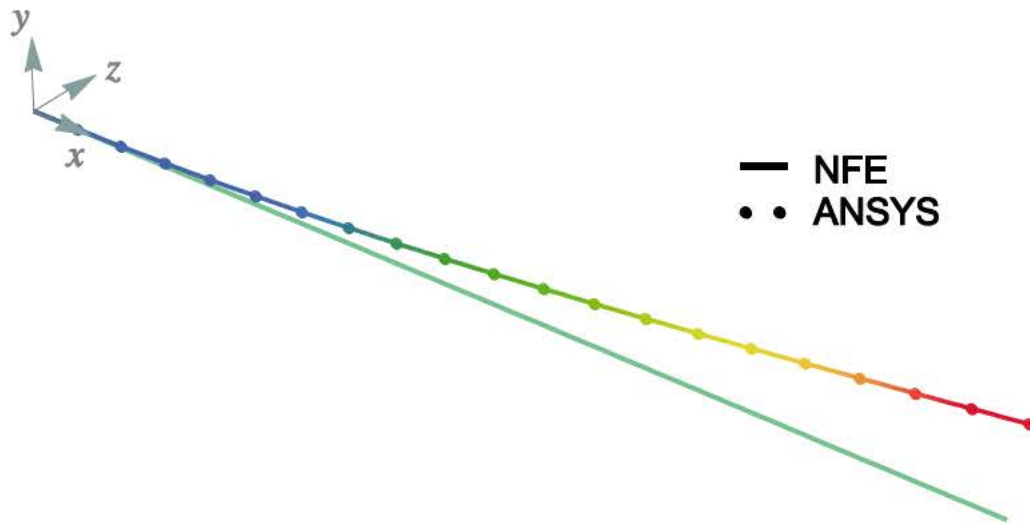


Figure 5: Total spatial deformation of FGM beam ( $F_x = 0$  N).

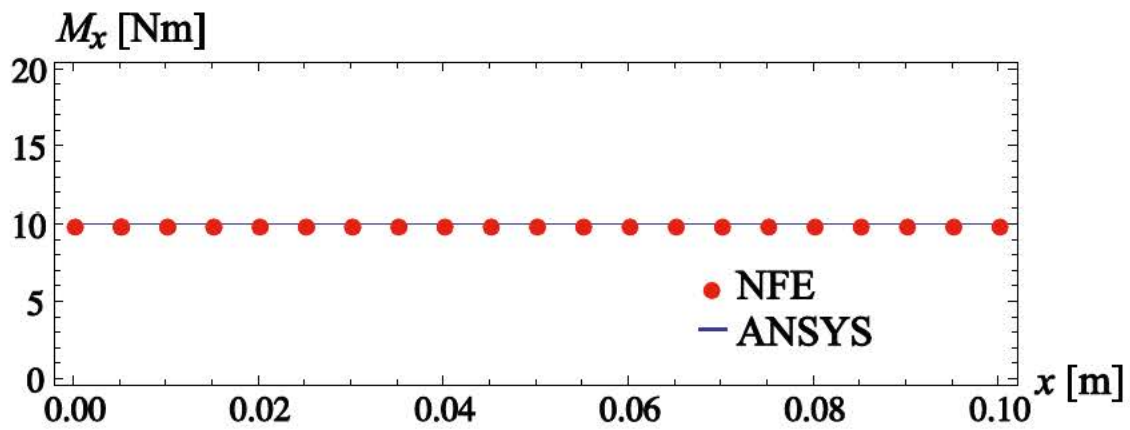


Figure 6: Torsion moment  $M_x(x)$ .

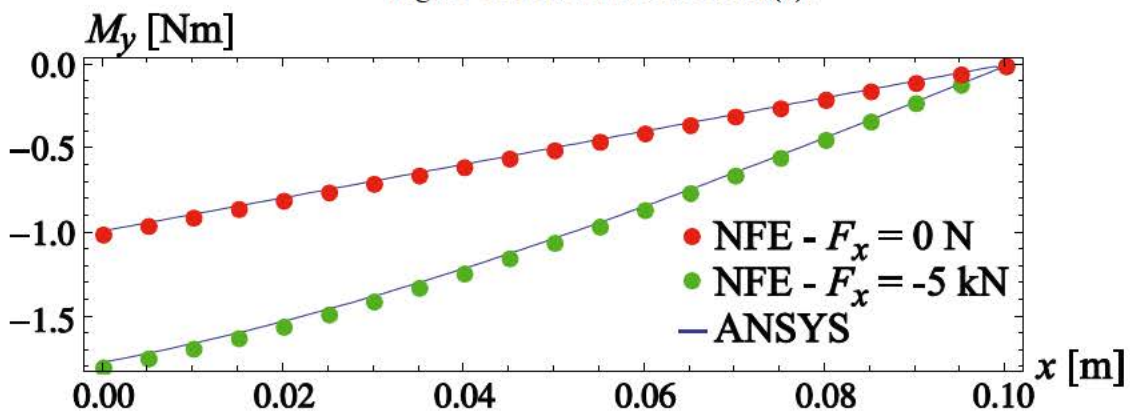


Figure 7: Bending moment about the  $y$ -axis.

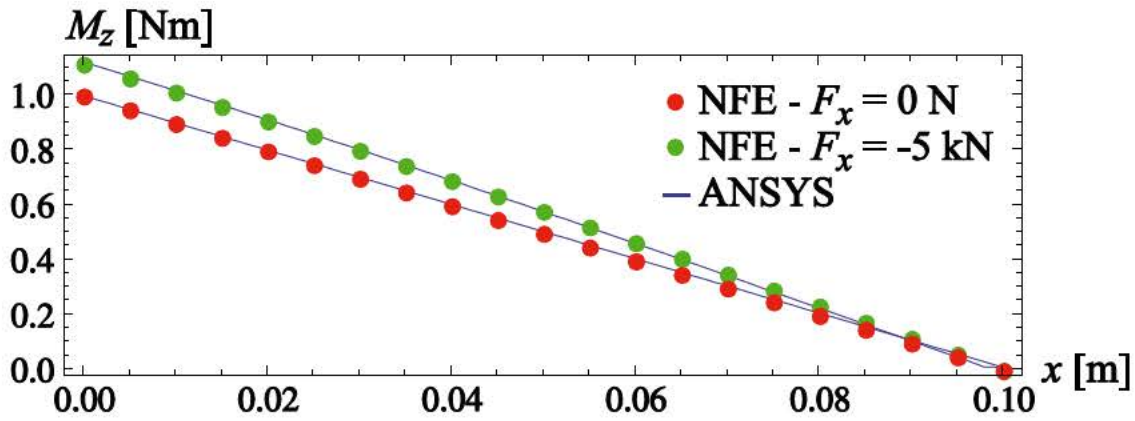


Figure 8: Bending moment about the  $z$  - axis.

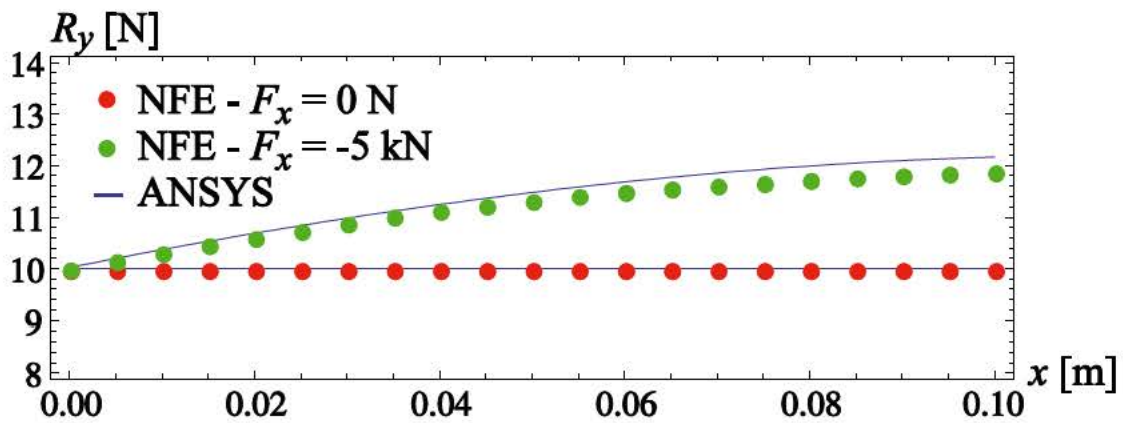


Figure 9: Transversal force in  $y$  - axis

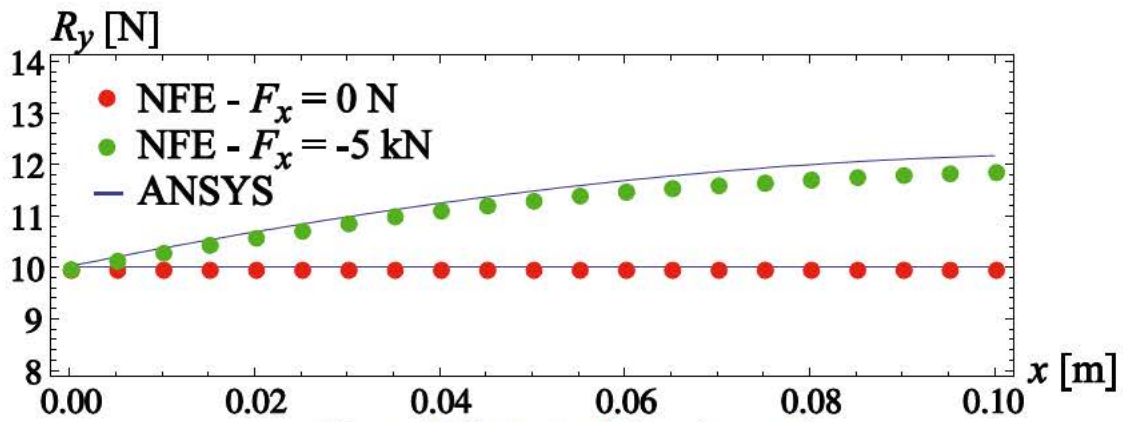


Figure 10: Transversal force in  $z$  - axis

#### 4.2 Example 2 - FGM beam structure-hollow cross-section

The FGM beam structure with a constant rectangular hollow cross-section is considered – Figure 11, which consists of two parts – Beam1 and Beam2. Its geometry is given with:  $h_1 = 0.005$  m,  $h_n = 0.00375$  m,  $b_1 = 0.01$  m,  $b_n = 0.0075$  m and  $L = 0.1$  m. The angle between the beams is  $\theta = 150^\circ$ . The cross-sectional area is  $A = 2.1875 \times 10^{-5}$  m<sup>2</sup>; the area moments of inertia are  $I_z = 7.12077 \times 10^{-11}$  m<sup>4</sup> and  $I_y = 2.84831 \times 10^{-10}$  m<sup>4</sup>, the cross-sectional area polar moment of inertia is  $I_p = I_y + I_z = 3.56038 \times 10^{-10}$  m<sup>4</sup> and the torsion constant is

$I_T = 1.6748 \times 10^{-10} \text{ m}^4$ . The FGM beam structure is loaded by the vertical force  $F_{ky} = -100 \text{ N}$  and the torsion moment  $M_{kx} = 100 \text{ Nm}$  at point  $k$ .

Material of the beams consists of two components: Aluminum Al6061-TO and titanium carbide TiC, that's material properties are the same as in the Example 1.

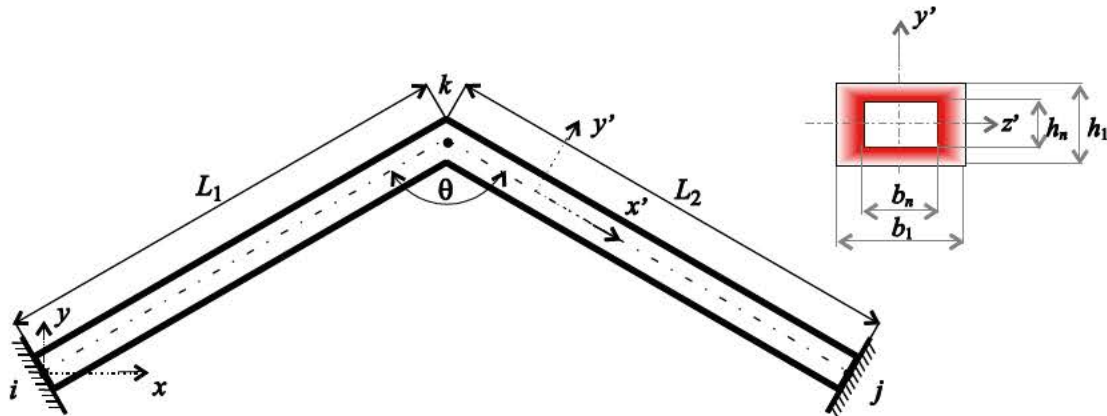


Figure 11: FGM beam structure.

The TiC volume fraction varies in the local  $y'$  and  $z'$  direction linearly and symmetrically according to the  $x' - y'$  and  $x' - z'$  planes:  $[v_f(y', z')]_{y'=\pm h_n/2} = 0$ ,  $[v_f(y', z')]_{z'=\pm b_n/2} = 1$ - the

inner edges of the cross-sectional area are made of pure Al6061-TO and the outer cross-section edges are made of pure fibre. Constant effective material properties are considered in the local  $x'$  - direction of both beams. Using EMR and MLM the effective elasticity modulus (in [GPa]) for axial loading  $E_L^{NH}$ , for bending about axis  $y'$  -  $E_L^{M_yH}$  and about axis  $z'$  -  $E_L^{M_zH}$  the shear moduli  $G_{Ly}^H$  and  $G_{Lz}^H$ , the torsional shear modulus have been calculated. The influence of the number of divisions  $n$  to the layers on the homogenized material properties are shown in Table 4. The shear correction factors  $k_y^{sm}$  and  $k_z^{sm}$  for  $n = 20$  layers are  $k_y^{sm} = 0.4712$  and  $k_z^{sm} = 0.2914$ .

Table 4: Influence of the number of divisions  $n$  to the layers on the homogenized material properties.

layers $n$	$E_L^{NH}$	$E_L^{M_yH} = E_L^{M_zH}$	$G_{Ly}^H = G_{Lz}^H$	$G_L^{M_xH}$
2	281.839	296.151	112.716	120.614
5	283.894	302.229	113.901	124.066
10	284.188	303.098	114.071	124.561
15	284.242	303.259	114.102	124.653
20	284.261	303.315	114.113	124.685

The FGM beam structure, clamped at the node  $i$  and  $j$ , is studied by elasto-static analysis. The effects of axial force is not considered by this example. The displacements according the global coordinate system at the point  $k$  are shown in Table 5 using the new FGM beam finite element (NFE) and homogenized material properties for  $n = 20$ . Only two of the herein proposed new FGM finite elements were used – one for each part. For comparison purposes, the same problem is solved using a very fine mesh – 21600 of SOLID186 elements of the

FEM program ANSYS [60]. The average relative difference  $\Delta$  [%] between displacements calculated by our method and the ANSYS solution is evaluated.

Table 5: Global displacements at point  $k$ .

Displacements [mm], [rad]	NFE without shear correction	NFE with shear correction	ANSYS	$\Delta$ [%] without shear correction	$\Delta$ [%] with shear correction
$v_k$	-0.01135	-0.01137	-0.01140	0.39	0.27
$w_k$	-2.56285	-2.56285	-2.58651	0.91	0.91
$\varphi_{xk}$	0.19804	0.19804	0.20030	1.13	1.13

The total deformation of the FGM beam structure is shown in Figure 12.

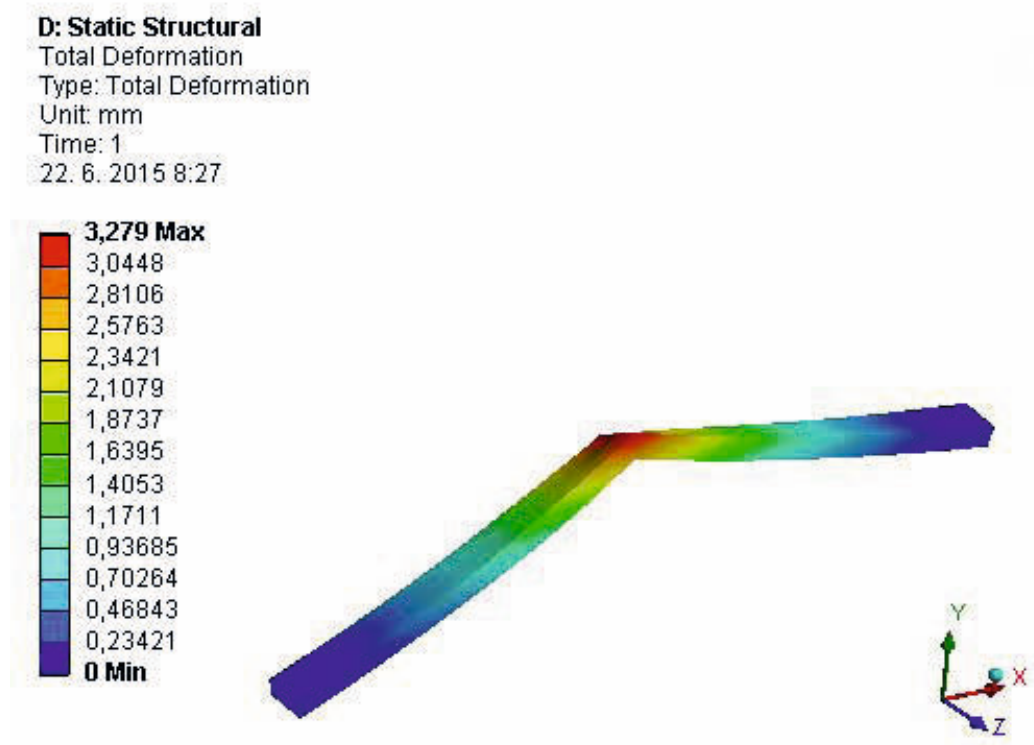


Figure 12: Total deformation of the FGM beam structure.

As can be seen in Table 4, a very good agreement of our results is obtained.

#### 4.3 Example 3 - FGM beam structure – square cross-section

The system of three FGM beams that joint points  $i = (0, 0, 0)$ ,  $j = (0.1, 0, 0)$ ,  $k = (0, 0, 0.1)$  and  $l = (0.05, 0.1, 0.05)$  is considered (Figure 13). The coordinates of the points are given in [m]. The square cross-section of all beams is constant with dimensions  $b = h = 0.01\text{m}$ .

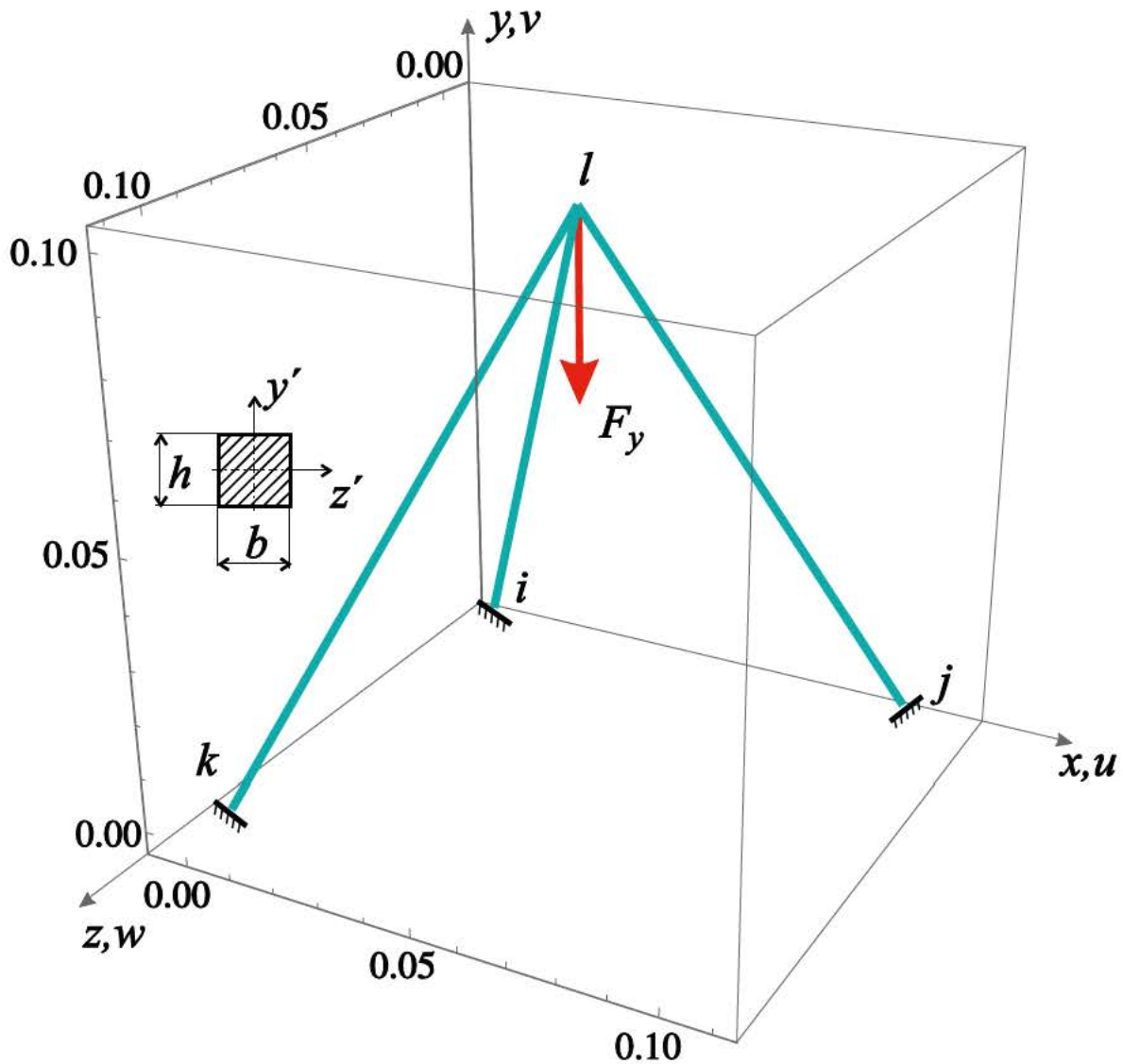


Figure 13: FGM beam structure.

The TiC volume fraction varies in the local  $y'$  and  $z'$  direction linearly and symmetrically according to the  $x' - y'$  and  $x' - z'$  planes:  $[v_f(y', z')]_{z'=0}^{y'=0} = 0$ ,  $[v_f(y', z')]_{z'=\pm b/2}^{y'=\pm h/2} = 1$  (similarly as in the Example 1) - the core of the beam is made from pure Al6061-TO and linearly varies to the edges that are made from pure TiC. Constant effective material properties are considered in the local  $x'$  - direction of all beams.

The average shear correction factor in  $y'$  - direction  $k_y^{sm} = 5/6$  and in  $z'$  - direction  $k_z^{sm} = 5/6$  is used assuming a constant Poisson ratio for simplicity. The beam structure is loaded by vertical force  $F_y = -100$  kN.

Using EMR and MLM the effective elasticity modulus for axial loading  $E_L^{NH}$ , for bending about axis  $y' - E_L^{M_yH}$  and about axis  $z' - E_L^{M_zH}$ , shear moduli  $G_{Ly}^H$  and  $G_{Lz}^H$ , and the torsional shear modulus  $G_L^{M_xH}$  have been calculated:

$$E_L^{NH} = 342.11 \text{ GPa}; \quad E_L^{M_yH} = E_L^{M_zH} = 396.43 \text{ GPa};$$

$$G_{Ly}^H = G_{Lz}^H = 138.58 \text{ GPa}; \quad G_L^{M,H} = 162.23 \text{ GPa};$$

The FGM beam structure clamped at the nodes  $i, j$  and  $k$  are studied by elasto-static analysis. The effect of axial force is not considered with in this example. The displacements according the global coordinate system are given in Table 6 using the new FGM beam finite element (only three finite elements are used). The same problem is solved using a mesh of 200 of BEAM188 elements of the FEM program ANSYS [60]. The average relative difference  $\Delta$  [%] between displacements calculated by our method and the ANSYS solution has been evaluated.

Table 6: Global displacements at node  $l$ .

Displacements [mm], [rad]	NFE	ANSYS	$\Delta$ [%]
$u_l$	0.2601	0.2606	0.21
$v_l$	-0.2601	-0.2606	0.21
$w_l$	0.2648	0.2651	0.10
$\varphi_{xl}$	0.00378	0.00375	0.73
$\varphi_{yl}$	0	0	0
$\varphi_{zl}$	-0.00378	-0.00375	0.73

As can be seen in Table 6, a very good agreement of both solution results has been obtained. The deformed FGM beam structure calculated by ANSYS and NFE is shown in Figure 14.

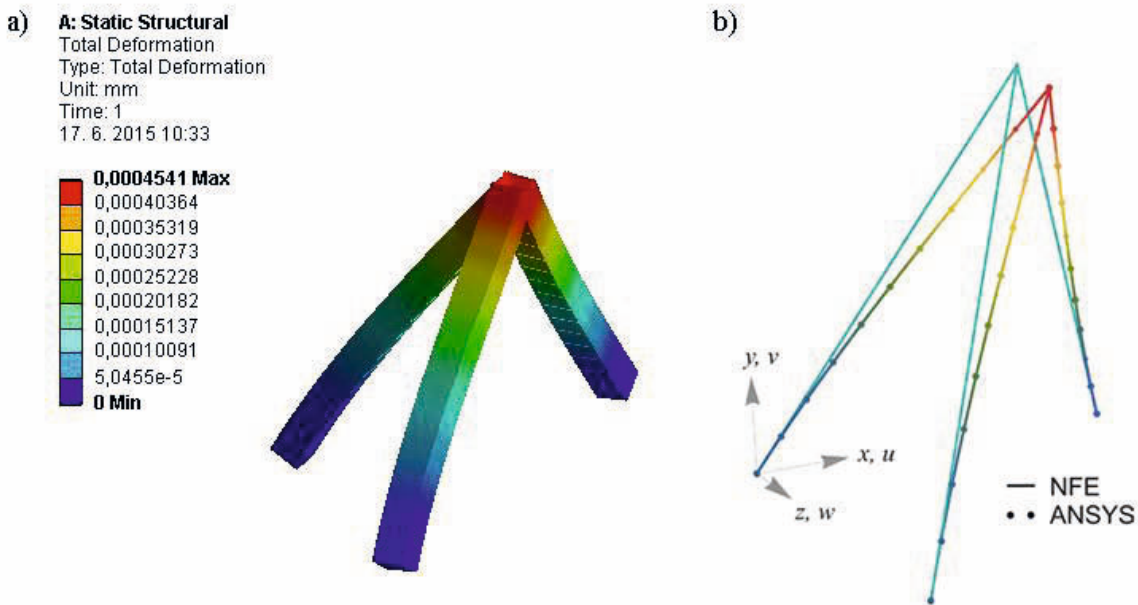


Figure 14: The deformed beam structure a) solution from ANSYS b) comparison of the ANSYS and NFE solution.

#### 4.4 Example 4 - FGM beam on vertical elastic foundation– spatial variation of material properties

The clamped FGM beam (at node  $i$ ) on varying vertical Winkler foundation has been considered (as shown in Figure 15). Its rectangular cross-section is constant with height  $h =$

0.005 m and width  $b = 0.01$  m. The length of the beam is  $L = 0.1$  m. Bending deformations of the beam are found.

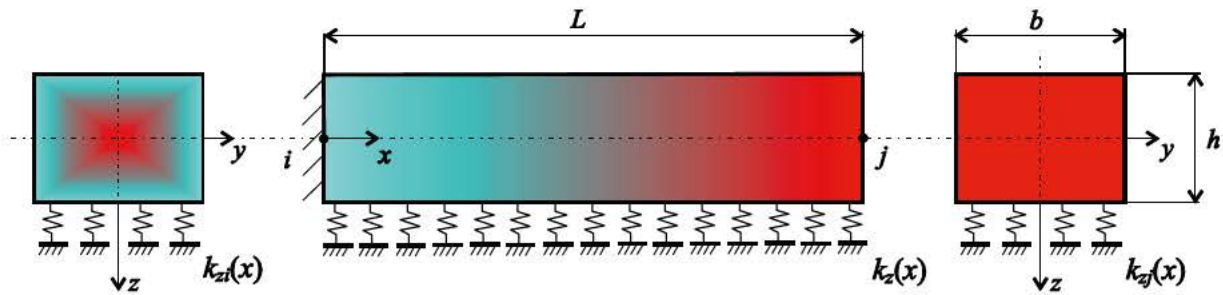


Figure 15: Clamped beam with spatially varying material properties.

The beam is made of a mixture of two components: Aluminum Al6061-TO and Titanium Carbide TiC, constant constituent's material properties are given in Example 1. The NiC volume fraction, in this case, varies linearly and symmetrically according to the  $x-y$  and  $x-z$  planes: At node  $i$  is  $[v_{fi}(y, z)]_{y=0}^{z=0} = 1$ ,  $[v_{fi}(y, z)]_{y=\pm h/2}^{z=\pm b/2} = 0$  and then vary continuous linearly in the longitudinal direction to the constant value at node  $j$  ( $v_{fj} = 1$ ).

Using EMR and MLM the effective elasticity modulus for axial loading -  $E_L^{NH}$ , for bending about axis  $y$  -  $E_L^{MyH}$  and about axis  $z$  -  $E_L^{MzH}$ , shear moduli  $G_{Ly}^H$  and  $G_{Lz}^H$ , and torsional shear modulus  $G_L^{MxH}$  are calculated:

$$E_L^{NH} = 342.109 - 2731.095x \text{ GPa};$$

$$E_L^{MyH} = E_L^{MzH} = 396.429 - 3274.293x \text{ GPa};$$

$$G_{Ly}^H = G_{Lz}^H = 138.581 - 1129.418x \text{ GPa};$$

$$G_L^{MxH} = 162.233 - 1362.936x \text{ GPa};$$

The FGM beam, clamped at the node  $i$ , resting on varying vertical Winkler elastic foundation  $k_z = 5000 - 30000x + 600000x^2$  kN/m<sup>2</sup> and loaded by forces  $F_y = F_z = 100$  N at node  $j$ , is studied by elasto-static analysis. The deformations at node  $j$  are evaluated using the new FGM beam finite element (NFE). Again, we only use one of the herein proposed finite elements. The effects of axial and shear forces were not considered in this example. The same problem is solved using a very fine mesh - 23015 of SOLID186 elements of the FEM program ANSYS [60]. The results of ANSYS as well as the results of the NFE are presented in Tables 7 and 8. The average relative difference  $\Delta$  [%] between displacements calculated by our method and the ANSYS solution is evaluated.

Table 7: Displacements at node  $j$  with and without shear correction factors (with elastic foundation).

Displacements at node $j$ [mm], [rad]	NFE without shear	NFE with shear	ANSYS	$\Delta$ [%] without shear	$\Delta$ [%] with shear
$v_j$	0.2690	0.27196	0.27513	2.29	1.17
$w_j$	0.4333	0.43508	0.43998	1.54	1.13

Displacements at node $j$ [mm], [rad]	NFE without shear	NFE with shear	ANSYS	$\Delta$ [%] without shear	$\Delta$ [%] with shear
$v_j$	0.2690	0.27196	0.27513	2.29	1.17
$w_j$	0.4333	0.43508	0.43998	1.54	1.13
$\varphi_{yj}$	-0.00867	-0.00870	-0.00903	4.02	3.67
$\varphi_{zj}$	0.00458	0.00461	0.00475	3.43	2.84

Table 8: Displacements at node  $j$  with and without elastic foundation.

Displacements at node $j$ [mm], [rad]	NFE with foundation	ANSYS with foundation	NFE without foundation	ANSYS without foundation
$v_j$	0.27196	0.27513	0.27196	0.27513
$w_j$	0.43508	0.43998	1.07584	1.08600
$\varphi_{yj}$	-0.00870	-0.00903	-0.01846	-0.01898
$\varphi_{zj}$	0.00461	0.00475	0.00462	0.00475

The comparison of the vertical beam deflection curve with and without elastic foundation is shown in Figure 16.

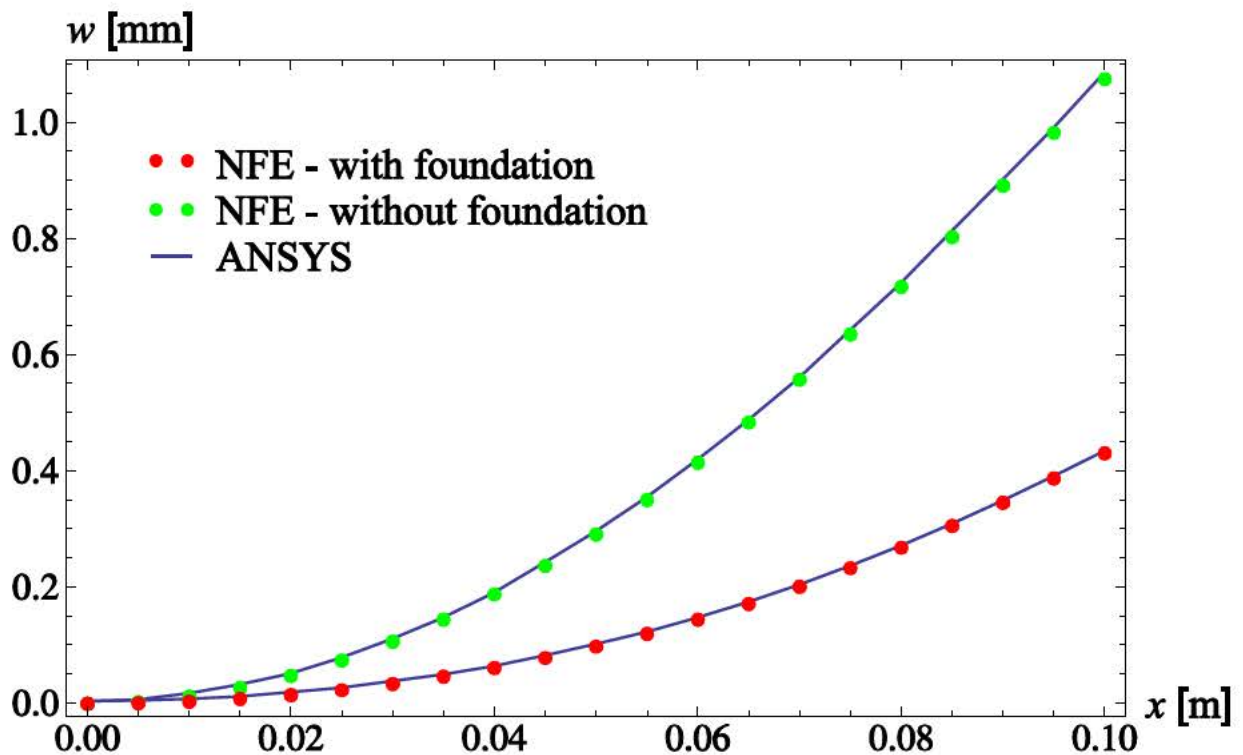


Figure 16: Comparison of the vertical beam deflection curve with and without elastic foundation.

Again, a good agreement of our results compared to ANSYS is indicated in Tables 7 and 8.

## 5 Conclusion

The new 3D beam finite element for elasto-static analysis of the FGM single beam and beam structures has been established in this contribution. Continuous transversal, lateral and longitudinal variation of material properties has been considered. Effect of varying Winkler elastic foundations and shear force deformation effect is taken into account. The effect of axial force has been taken into account for the flexural loading. The axial force has a system character: if we set it to zero, the 1st order beam theory is obtained. The axial force of the 2nd order beam theory can be practically induced with structural, thermal or electro-magnetic loads. In analysis of a single straight beam the global finite element matrix coincides with the derived local finite element matrix. The global matrix of beam structures can be generally established by classical methods. For an elastic-static analysis, the load vector has to be established and applied. The obtained results have been studied and compared with results obtained using very fine continuum and beam meshes by the FEM program ANSYS. An excellent agreement of our solution results is obtained, which confirms respectable accuracy and effectiveness of our approach.

## Acknowledgement

This work was financially supported by grants of Science and Technology Assistance Agency no. APVV-0246-12 and Scientific Grant Agency of the Ministry of Education of Slovak Republic and the Slovak Academy of Sciences and VEGA No. 1/0453/15.

Authors are also grateful to the HPC Center at the Slovak University of Technology in Bratislava, which is a part of the Slovak Infrastructure of High Performance Computing (SIVVP project, ITMS code 26230120002, funded by the European Regional Development Funds), for the computational time and resources made available.

## REFERENCES

- [1] Birman, V., Byrd, L.W. Modeling and analysis of functionally graded materials and structures. *Applied mechanics reviews* (2007) **60**: 195-216.
- [2] Ying, J., Lu, C.F., Chen, W.Q. Two –dimensional elasticity solutions for functionally graded beams resting on elastic foundation. *Composite Structures* (2008) **84**: 209-219.
- [3] Benatta, M.A, Mechab, I., Tounsi, A., Adda Bedia, E.A. Static analysis of functionally graded short beams including warping and shear deformation effects. *Computational Materials Science* (2008)**44**: 765-773.
- [4] Kadoli, R., Akhtar, K., Ganesan, N. Static analysis of functionally graded beams using high order shear deformation theory. *Applied Mathematical Modelling* (2008) **32**: 2509-2525
- [5] Giunta, G., Belouettar, S., Carrera, E. Analysis of FGM Beams by Means of Classical and Advanced Theories. *Mechanics of Advanced Materials and Structures* (2010) **17**: 622-635.
- [6] Kang. Y.A., Li, X.F. Large Deflections of a Non-linear Cantilever Functionally Graded Beam. *Journal of Reinforced Plastics and Composites* (2010) **29**: 1761-1774.
- [7] Huang, Y., Li, X.F. Buckling Analysis of Nonuniform and Axially Graded Columns with Varying Flexural Rigidity. *Journal of Engineering Mechanics – ASCE* (2011) **137**: 73-81.
- [8] Asghari, M., Rahaeifard, M., Kahrobaiyan M.H., Ahmadian, M.T. The modified couple stress functionally graded Timoshenko beam formulation. *Material and Design* (2011) **32**: 1435-1443

- [9] Kocaturk, T., Simsek, M., Akbas, S.D. Large displacement static analysis of a cantilever Timoshenko beam composed of functionally graded material. *Science and Engineering of Composite Materials* (2011) **18**: 21-34.
- [10] Mohanty, C.S., Dash, R.R., Rout, T. Parametric instability of a functionally graded Timoshenko beam on Winkler's elastic foundation. *Nuclear Engineering and Design* (2011) **241**: 2698-2715.
- [11] Ma, L.S., Lee, D.W. Exact solutions for nonlinear static responses of a shear deformable FGM beam under an in-plane thermal loading. *European Journal of Mechanics A/Solids* (2012) **31**: 13-20.
- [12] Mena, R., Tounsi, A., Mouaici, F., Mechab, I., Zidi, M., Bedia, E.A.A. Analytical Solutions for Static Shear Correction Factor of Functionally Graded Rectangular Beams. *Mechanics of Advanced Materials and Structures* (2012) **19**: 641-652.
- [13] Zhou, Li, S.R., Wan, Z.Q., Zhang, P. Relationship between Bending Solutions of FGM Timoshenko Beams and Those of Homogenous Euler-Bernoulli Beams. *Applied Mechanics and Materials: Progress in Structures, PTS 1-4* (2012) **166-169**: 2831-2836.
- [14] Soleimani, A., Saadatfar, M. Numerical Study of Large Deflection of Functionally Graded Beam with geometry Nonlinearity. *Advanced Material Research: MEMS, Nano and Smart Systems, PTS 1-6* (2012) **403-408**: 4226-4230
- [15] Birsan, M., Altenbach, H., Sadowski, T., Eremeyev, V.A., Pietras, D. deformation analysis of functionally graded beams by the direct approach. *Composites: Part B* (2012) **43**: 1315-1328
- [16] Mohanty, S.C., Dash, R.R., Rout, T. Static and Dynamic Stability of Functionally Graded Timoshenko Beam. *International Journal of Structural Stability and Dynamics* (2012) **12**.
- [17] Zhao, L., Chen, W.Q., Lu, C.F. Symplectic elasticity for bi-directional functionally graded materials. *Mechanics of Materials* (2012) **54**: 32-42.
- [18] Esfahani, S.E., Kiani, Y., Eslami, M.R. Non-linear stability thermal analysis of temperature dependent FGM beams supported on non-linear hardening elastic foundations. *International Journal of Mechanical Science* (2013) **69**: 10-20
- [19] Ansari, R., Gholami, R., Faghieh Shojaei, M., Mohammadi, V., Sahmani, S. Size-dependent bending, buckling and free vibration of functionally graded Timoshenko microbeams based on the most general strain gradient theory. *Composite Structure* (2013) **100**: 385-397.
- [20] Zhang, Da-Guang. Nonlinear bending analysis of FGM beams based on physical neutral surface and high order shear deformation theory. *Composite Structures* (2013) **100**: 121-126.
- [21] Li, S.R., Cao, D.F, Wan, Z.Q. Bending solutions of FGM Timoshenko beams from those of the homogenous Euler-Bernoulli beams. *Applied Mathematical Modelling* (2013) **37**: 7077-7085.
- [22] Zamanzadeh M., Rezazadeh G., Jafarsadeghi-poornaki, I., Shabani, R. Static and dynamic stability modeling of a capacitive FGM micro-beam in presence of temperature changes. *Applied Mathematical Modelling* (2013) **37**: 6964-6978.
- [23] Mao, Y.Q., Ai, S.G., Fang, D.N., Fu, Y.M, Chen, C.P. Elasto-plastic analysis of micro FGM beam basing on mechanism-based strain gradient plasticity theory. *Composite Structures* (2013) **101**: 168-179.
- [24] Abbasnejad, B., Rezazadeh, G., Shabani, R. Stability Analysis of a Capacitive FGM Micro-Beam using Modified Couple Stress Theory. *ACTA Mechanica Solida Sinica* (2013) **26**: 427-440.
- [25] Akgoz, B., Civalek, O. Buckling analysis of functionally graded microbeams based on the strain gradient theory. *Acta Mechanica* (2013) **224**: 2185-2201.
- [26] Zhang, B., He, Y., Liu, D., Gan, Z., Shen, L. A novel size-dependent functionally graded curved microbeam model based on the strain gradient elasticity theory. *Composite Structures* (2013) **106**: 374-392.
- [27] Zhang, D.G. Thermal post-buckling and nonlinear vibration analysis of FGM beams based on physical neutral surface and high order shear deformation theory. *Meccanica* (2014) **49**: 283-293.

- [28] Li, Y.L., Meguid, S.A., Fu, Y.M., Xu, D.L. Nonlinear analysis of thermally and electrically actuated functionally graded material microbeam. *Proceedings of the Royal Society a Mathematical Physical and Engineering sciences* (2014) **470**.
- [29] Shen H-S., Wang, Z-X. Nonlinear analysis of shear deformable FGM beams resting on elastic foundation in thermal environments. *International Journal of Mechanical Sciences* (2014) **81**: 195-206.
- [30] Hadji, L., Daouadji, T.H., Tounsi, A., Bedia, E.A. A higher order shear deformation theory for static and free vibration of FGM beam. *Steel and Composite Structures* (2014) **16**: 507-519.
- [31] Nguyen, D.K., Gan, B.S., Trinh, T.H. Geometrically nonlinear analysis of planar beam and frame structures made of functionally graded material. *Structural Engineering and Mechanics* (2014) **49**: 727-743.
- [32] Zhang, D.G., Zhou, H.M. Nonlinear Bending and Thermal Post-Buckling Analysis of FGM Beams Resting on Nonlinear Elastic Foundation. *CMES – Computer Modelling in Engineering & Science* (2014) **100**: 201-222.
- [33] Sitar, M., Kosel, F., Brojan, M. Large deflections of nonlinearly elastic functionally graded composite beams. *Archives of Civil and Mechanical Engineering* (2014) **14**: 700-709.
- [34] Cai, K., Gao, D.Y., Qin, Q.H. Postbuckling analysis of a nonlinear beam with axial functionally graded material. *Journal of Engineering Mathematics* (2014) **88**: 121-136.
- [35] Chu, P., Li, X.-F., Wang, Z.-G., Lee, K.Y. Double cantilever beam model for functionally graded materials based on two-dimensional theory of elasticity. *Engineering Fracture Mechanics* (2015) **135**: 232-244.
- [36] Filippi, M., Carrera, E., Zenkour, A.M. Static analyses of FGM beams by various theories and finite elements. *Composites: Part B* (2015) **72**: 1-9.
- [37] Chakraborty, A., Gopalakrishnan, S., Reddy, J.N. A new beam finite element for the analysis of functionally graded materials. *International Journal of Mechanical Sciences* (2003) **45**: 519-539.
- [38] Alshorbagy A.E., Eltahir, M.A., Mahmoud F.F. Free vibration characteristics of a functionally graded beam by finite element. *Applied Mathematical Modelling* (2011) **35**: 412-425.
- [39] Murin, J., Aminbaghai M., Kutis, V. Exact solution of the bending vibration problem of the FGM beam with variation of material properties. *Engineering Structures* (2010) **32**: 1631-1640.
- [40] Aminbaghai, M., Murin, J., Kutis V. Modal analysis of the FGM-beams with continuous transversal symmetric and longitudinal variation of material properties with effect of large axial force. *Engineering Structures* (2012)**34**: 314-329.
- [41] Murin, J., Aminbaghai, M., Kutis, V., Hrabovsky, J. Modal analysis of the FGM beams with effect of axial force under longitudinal variable elastic Winkler foundation. *Engineering Structures* (2013) **49**: 234-247.
- [42] Murin, J., Aminbaghai, M., Hrabovsky, J., Kutis, V., Kugler St. Modal analysis of the FGM beams with effect of the shear correction function. *Composites: Part B* (2013) **45**:1575–1582.
- [43] Kutis, V., Murin, J., Belak, R., Paulech, J. Beam element with spatial variation of material properties for multiphysics analysis of functionally graded materials. *Computers and Structures* (2011)**89**: 1192 – 1205.
- [44] Rubin, H. Analytische Berechnung von Stäben und Stabwerken mit stetiger Veränderlichkeit von Querschnitt, elastischer Bettung und Massenbelegung nach Theorie erster und zweiter Ordnung, Baustatik - Baupraxis 7. Berichte der 7. Fachtagung "Baustatik - Baupraxis" Aachen/Deutschland 18.-19. März 1999. Balkema 1999, Abb., Tab.S.135-145.
- [45] Rubin, H. Solution of differential equations of arbitrary order with polynomial coefficients and application to a statics problem *ZAMM* (1996)**76**: 105-117.
- [46] S. Wolfram MATHEMATICA 5, Wolfram research, Inc., 2003.
- [47] Altenbach, H., Altenbach, J., Kissing, W. *Mechanics of composite structural elements*. Springer Verlag, (2003).

- [48] Halpin, J.C., Kardos, J.L. The Halpin-Tsai equations. A review, *Polymer Engineering and Science*. (1976) **16**: 344-352.
- [49] Reuter, T., Dvorak, G.J. Micromechanical models for graded composite materials: II. Thermomechanical loading. *J. of the Mechanics and Physics of Solids* (1998) **46**:1655-1673.
- [50] Murin, J., Kutis, V. Improved mixture rules for composite (FGMs) sandwich beam finite element. In *Computational Plasticity IX. Fundamentals and Applications*. Barcelona, Spain, (2007): 647-650.
- [51] Alshorbagy, A.E., Eltaher, M.A., Mahmoud F.F. Free vibration of a functionally graded beam by finite element method. *Applied Mathematical Modelling* (2010) **35**: 412 – 425.
- [52] Simsek, M. Vibration analysis of a functionally graded beam under a moving mass by using different beam theories, *Composite Structures* (2010) **92**: 904-917.
- [53] Rout, T. On the dynamic stability of functionally graded material under parametric excitation. PhD thesis. National Institute of Technology Rourkela, India. (2012).
- [54] Kutis, V., Murin, J., Belak, R., Paulech, J. Beam element with spatial variation of material properties for multiphysics analysis of functionally graded materials. *Computers and Structures* (2010) **89**: 1192-1205.
- [55] Murin, J., Kugler, S., Aminbaghai, M., Hrabovsky, J., Kutis, V., Paulech, J. *Homogenization of material properties of the FGM beam and shells finite elements*. In.: 11<sup>th</sup> World Congress on Computational mechanics (WCCM XI), Barcelona, 2014.
- [56] Murin, J., Aminbaghai, M., Hrabovsky, J., Kutis, V., Paulech, J., Kugler, S. *A new FGM beam finite element for modal analysis*. In.: 11<sup>th</sup> World Congress on Computational mechanics (WCCM XI), Barcelona, 2014.
- [57] Murin, J., Kugler, S., Aminbaghai, M., Hrabovsky, J., Kutis, V., Paulech, J. *Homogenization of material properties of the FGM beam and shell finite elements*. In.: 11<sup>th</sup> World Congress on Computational mechanics (WCCM XI), Barcelona, 2014.
- [58] Murin, J., Hrabovský, J., Kutiš, V., Paulech, J. *Shear correction function derivation for the FGM beams*. In: 2nd International Conference on Multi-scale Computational Methods for solid and Fluids. 10. 6– 12. 6.2015, Sarajevo, Bosnia and Hercegovina, (2015).
- [59] Murin, J., Aminbaghai, M., Hrabovsky, J., Kutis, V. Kugler, S. *Effect of the Shear Correction Function in the FGM Beams Modal Analysis*. In Proceedings of the 15th European Conference on Composite Materials. 24-28 June 2012, Venice, Italy, (2012) ISBN 978-88-88785-33-2.
- [60] ANSYS Swanson Analysis System, Inc., 201 Johnson Road, Houston, PA 15342/1300, USA.

